
2.4 Hot-Gas Cleanup

HOT-GAS CLEANUP

**Semiannual Technical Progress Report
for the Period January 1, 1992 - June 30, 1992**

by

**Michael L. Jones, CESRI Director
Jay S. Haley, Research Engineer
John Hurley, Research Supervisor
Blazo Ljubcic, Research Engineer
Murali Ramanathan, Research Scientist**

**Energy and Environmental Research Center
University of North Dakota
Box 8213, University Station
Grand Forks, ND 58202-8213**

Technical Monitor: Richard A. Dennis

for

**U.S. Department of Energy
Morgantown Energy Technology Center
3610 Collins Ferry Road
P.O. Box 880, Mail Stop E02
Morgantown, WV 26507-0880**

July 1992

Work Performed Under Cooperative Agreement No. DE-FC21-86MC10637

TABLE OF CONTENTS

	<u>Page</u>
LIST OF FIGURES	ii
LIST OF TABLES	iii
1.0 INTRODUCTION	1
2.0 GOALS AND OBJECTIVES	1
3.0 PROJECT DESCRIPTION	1
4.0 ACCOMPLISHMENTS	2
4.1 Particulate Control	2
4.2 Pressurized Drop-Tube Furnace	13
4.3 Thermochemical Equilibrium Modeling: PHOEBE Database Modifications	26
4.3.1 Database Format Change	27
4.3.2 Additions to Database	28
4.3.3 Database Utilities	30
4.4 PHOEBE Algorithm Extensions	32
4.4.1 Original Algorithm Description	32
4.4.2 Pressure Calculations	34
4.4.3 Preprocessor Utilities	35
4.4.4 Tests of the Database Algorithms	37
5.0 FUTURE WORK	37
5.1 Particulate Control	37
5.2 Alkali Gettering	39
5.3 Thermochemical Modeling	39
6.0 REFERENCES	39
APPENDIX A	A-1
APPENDIX B	B-1

LIST OF FIGURES

<u>Figure</u>	<u>Page</u>
1 Hot-gas cleanup test loop.	3
2 Nitrogen pressure variation ($p_{initial} = 18$ psi).	5
3 Nitrogen pressure variation ($p_{initial} = 37$ psi).	5
4 Nitrogen pressure variation ($p_{initial} = 60$ psi).	6
6 Infinite pulse ($p_{initial} = 37$ psi).	7
7 Infinite pulse ($p_{initial} = 60$ psi).	7
8 Backpulse gas temperature in front of the filter ($p_{initial} = 18$ psi).	8
9 Backpulse gas temperature in front of the filter ($p_{initial} = 37$ psi).	8
10 Backpulse gas temperature in front of the filter ($p_{initial} = 60$ psi).	9
11 Pressure wave intensity in front of the filter ($p_{initial} = 18$ psi).	10
12 Pressure wave intensity in front of the filter ($p_{initial} = 37$ psi).	10
13 Pressure wave intensity in front of the filter ($p_{initial} = 60$ psi).	11
14 Particulate sampling system	12
15 Pressurized drop-tube furnace process schematic.	15
16 Furnace assembly in PDTF vessel.	16
17 Photograph of PDTF pressure vessel.	17
18 Photograph of PDTF translating mechanisms.	18
19 Schematic of PDTF sampling probe with interchangeable tips.	19
20 Schematic of coal feeder for pressurized drop-tube furnace.	20
21 The percent of the total ash collected in each size fraction for the tests of kaolin as an alkali getter.	22
22 The major element composition of the ash collected in each size fraction for the tests of kaolin as an alkali getter.	24
23 The weight percent of each element collected in each size fraction for the tests of kaolin as an alkali getter.	25
24 An example system definition tree (SDT)	36

LIST OF FIGURES (Continued)

	<u>Page</u>
25 A plot of the experimental PHOEBE-predicted phase diagram for $\text{Al}_2\text{O}_3\text{-SiO}_2$	38
26 A plot of the experimental vs. predicted phase diagram for Na_2SiO_4	38

LIST OF TABLES

<u>Table</u>		<u>Page</u>
1	Specifications for an Isokinetic Particulate Sampling System . . .	11
2	Average Test Conditions for Alkali Gettering Tests in the EERC Pressurized Drop-Tube Furnace System	21
3	Field Identifier Prefixes (FIPs) and Explanations	28
4	PHOEBE Database: Record Entry for Aluminum	29

HOT-GAS CLEANUP

1.0 INTRODUCTION

The U.S. Department of Energy (DOE) is promoting the development of coal-based advanced power systems under the direction of the Morgantown Energy Technology Center (METC). This activity covers a broad range of technologies involving combustion, gasification, and the integration of combustion and gasification technologies. The objective is to maximize cycle efficiencies to provide for a stable, secure, and environmentally sound energy future.

Specific combustion program areas include the development of heat engines such as direct coal-fired turbines and diesels and pressurized fluidized-bed combustion (PFBC). Gasification technology development includes mild gasification for coproducts and hydrogen and methane production for fuel cell applications. Integrated gasification combined cycle (IGCC) technology promotes high cycle efficiencies by combining coal gasification with direct product-gas firing in turbines. In all of these cases, hot-gas cleanup systems are required to achieve acceptable process performance and to meet current and future environmental emission standards.

2.0 GOALS AND OBJECTIVES

The goals of the hot-gas cleanup project at the Energy and Environmental Research Center (EERC) are to build and operate a hot-gas cleanup test loop in conjunction with various pilot-scale advanced systems currently in operation at the Center and to explore the various ash/alkali corrosion mechanisms for ceramic barrier filter materials and to determine the effects of various mitigation options. The mitigation options will focus primarily on gettinger techniques. Eventually these techniques will be verified at the pilot scale using the hot-gas test loop.

The Center is currently operating the following pilot-scale fluidized-bed reactors:

- Fluidized-bed mild gasification reactor
- Fluidized-bed catalytic reactor for the production of hydrogen
- Pressurized fluidized-bed combustor

The Center is also planning to install and operate a transport reactor test unit (TRTU) to provide scaleup data for the hot-gas cleanup test facility in Wilsonville, Alabama.

3.0 PROJECT DESCRIPTION

The Energy and Environmental Research Center is currently involved in a number of research projects in both the combustion and gasification of coal and also in gas-stream cleanup. The fundamental gas-stream cleanup issues common to the various advanced concept systems are being investigated in this

project. Emphasis is being placed on particulate control techniques and on ash/alkali interactions with the filter materials.

In order to investigate particulate control methods, a test loop was constructed and inserted into the exhaust piping of the advanced concept reactors at the Center. The test loop provides a means of exposing various hot-gas cleanup systems to actual product gases from coal gasification and combustion using fluidized-bed reactors. Long-term effects on hot-gas cleanup systems can be studied economically by passively participating in the various research gasification and combustion runs. Filter efficiency, strength degradation, changes in permeability, and corrosion resistance are being investigated, as well as other pertinent issues such as cleaning techniques and temperature/pressure effects.

The Center has been involved in research related to ash/alkali interactions and slag behavior for many years. This expertise is being used in studying the effects of alkali interactions with filter media and possible mitigation options that may improve filter life. The global or overall objective in this phase of the project is the study of the thermodynamically equilibrated reaction mechanisms and mineral matter transformations in advanced coal combustion systems.

During this reporting period, bench-scale tests of kaolin as an entrained alkali getter in atmospheric and pressurized coal combustion conditions were performed. In addition, software was improved to permit a computer model study of other possible getters and getter concentrations.

The thermochemical equilibrium calculation package PHOEBE, developed at the EERC, was selected as the software tool to perform this study. After a careful review of the current state of development of PHOEBE, two major components of the package were identified as being critical to the applicability of the package to advanced coal combustion systems and in need of further development.

A framework for the requisite development was established. This framework was comprised of two tasks. The first was to address the enlargement of the database component of PHOEBE so that chemical species characteristic of advanced coal combustion systems would be well represented in the database. The second was set up to address the algorithmic aspects of the package so that the equilibrium computations would be pressure-dependent. (Since the system pressure is a critical operational parameter, sensitivity to variations in pressure is required of any equilibrium computation package used in this context.)

4.0 ACCOMPLISHMENTS

4.1 Particulate Control

A hot-gas cleanup test loop has been designed and constructed for use with each of the three reactors (Figure 1). The test loop was constructed using high-alloy metals with no refractory in order to minimize maintenance and to avoid ash/alkali/refractory interactions that may occur due to the high surface-to-volume ratio present in smaller-scale systems. The alloys used in construction were Haynes alloys HR-160 and 556, and 316H stainless steel. The

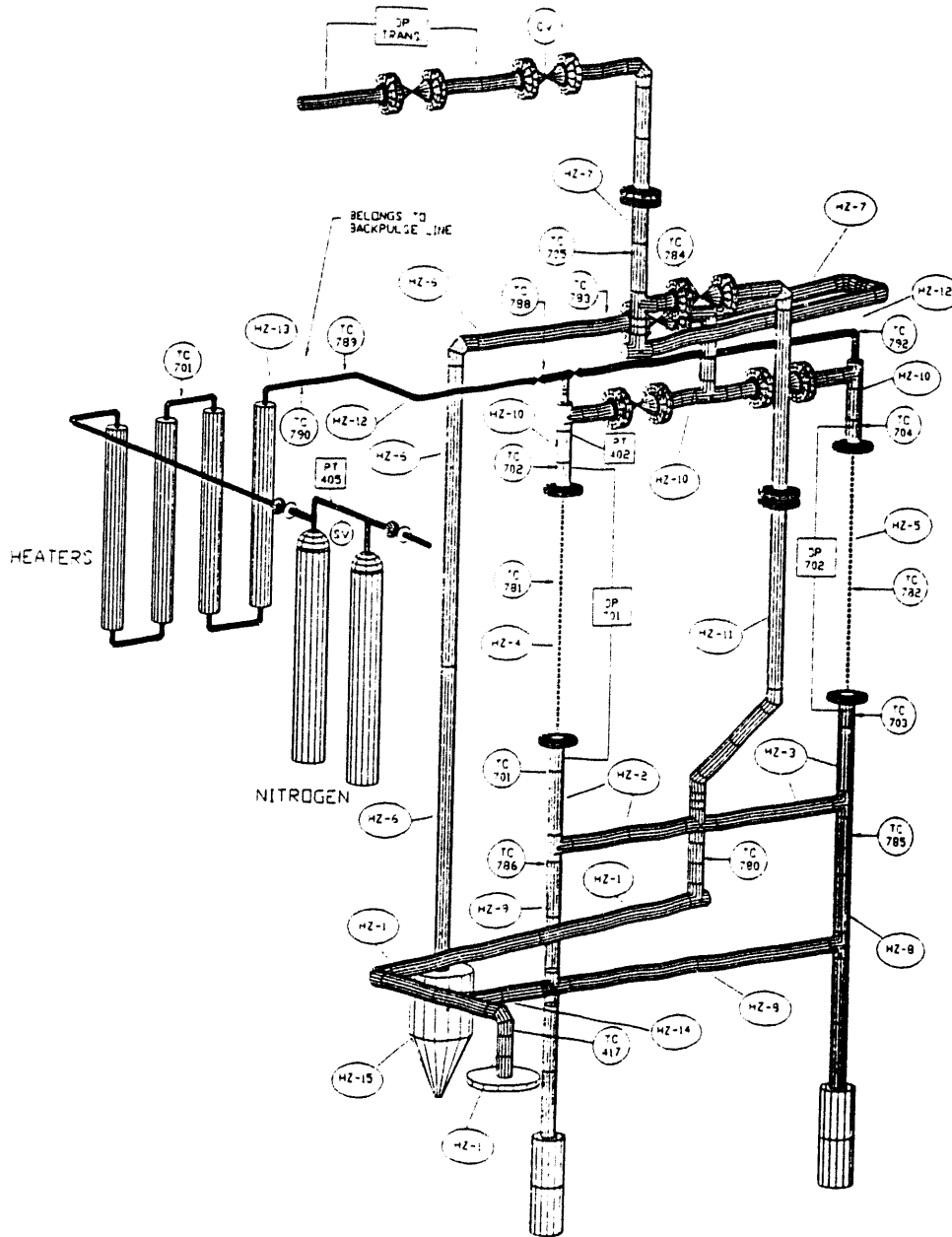


Figure 1. Hot-gas cleanup test loop.

piping used in the highest-temperature regions was HR-160 and 556. It is expected that these alloys will demonstrate good high-temperature corrosion characteristics under both oxidizing and reducing conditions. The test loop is designed to operate at temperatures up to 1650°F and pressures up to 150 psig. The system was designed in accordance with B31.3 piping codes. The test loop consists of a single inlet pipe which branches into three different flow paths. Each path is controlled by a high-temperature valve located as far downstream as possible in order to minimize thermal stresses in the valves. Two of the flow paths are identical and are used as filter element test bays, and the third branch is used as a bypass line. Filter elements can be installed in either or both test bays simultaneously. The filter modules are flange-mounted so that they may be replaced as necessary for different

filter types. The flanges used currently will permit operating conditions up to 1500°F and 150 psig. In order to achieve operating conditions up to 1650°F and 150 psig, further engineering is required to ensure that the flanged connection satisfies the criteria of the B31.3 piping code. The system will not be operated above 1500°F and 150 psig until this work has been completed. Gas flow rates through the various paths can be regulated by the downstream valves. The piping system is heated electrically using guard heaters. Pipe temperatures can be maintained at 1650°F continuously so that the process gas temperature can be raised or maintained as required in order to simulate the desired hot-gas conditions. The system has a heated backpulse system capable of delivering pressurized, heated, inert gas to the filter modules for cleaning purposes. The inlet piping to the test loop can be connected to a 100-lb/hr fluidized-bed gasifier or to other reactors being used for research at the Center. The TRTU is expected to be operational sometime in early 1993 and will be installed near the 100-lb/hr fluidized-bed reactor. The test loop will be connected to the TRTU when it is ready for operation.

To effectively use filter elements for a given application, many variables need to be considered, including system temperature, system pressure, initial clean pressure drop, total allowable pressure drop, system flow rate, etc. Any combination of these factors can affect the resulting filter efficiency.

Before a final parametric study was performed to define the characteristics of unsteady flow associated with the heated nitrogen backpulse system, research was conducted on the cleanup system. The goal was to determine backpulse operating range (minimum and maximum pulse duration) and to define solenoid valve operating policy that will maximize nitrogen backpulse cleaning efficiency.

Operating policy was specified by nitrogen pressure and backpulse duration. Three levels of nitrogen pressure were analyzed: 18, 37, and 60 psi. Pulse duration was controlled by a computer-controlled solenoid valve. Valve-opening duration was increased from 0.1 to 1 sec, with time increments of 0.1 sec; from 1 to 2 sec, with time increments of 0.25 sec; and from 2 to 3 sec, with time increments of 0.5 sec. Finally, the solenoid valve was opened for 90 sec, and nitrogen temperature versus time dependence was determined. For all tests, pressure and temperature at the points relevant to filter behavior over the observation periods were recorded and data stored in a computer.

Nitrogen pressure variation as a function of time and pulse duration is shown in Figures 2 through 4. For all three different initial pressure levels, minimum pressure reached was a strong function of pulse duration: the longer the pulse, the lower the minimum system pressure observed. Tests with the solenoid valve permanently open indicate that minimum pressure was reached in a maximum 8-sec period for all pressure levels (see Figures 5 through 7).

Backpulse gas temperature at the front of the filter for three different pressure levels is shown in Figures 8 through 10. Results indicate that pulse durations less than 2 sec were not long enough to ensure that the maximum temperature was reached. A higher initial pressure level resulted in a higher maximum gas temperature reached at the front of the filter. Infinite pulse tests showed that, once maximum temperature was reached, it remained constant as long as the solenoid valve was open (Figures 5 through 7).

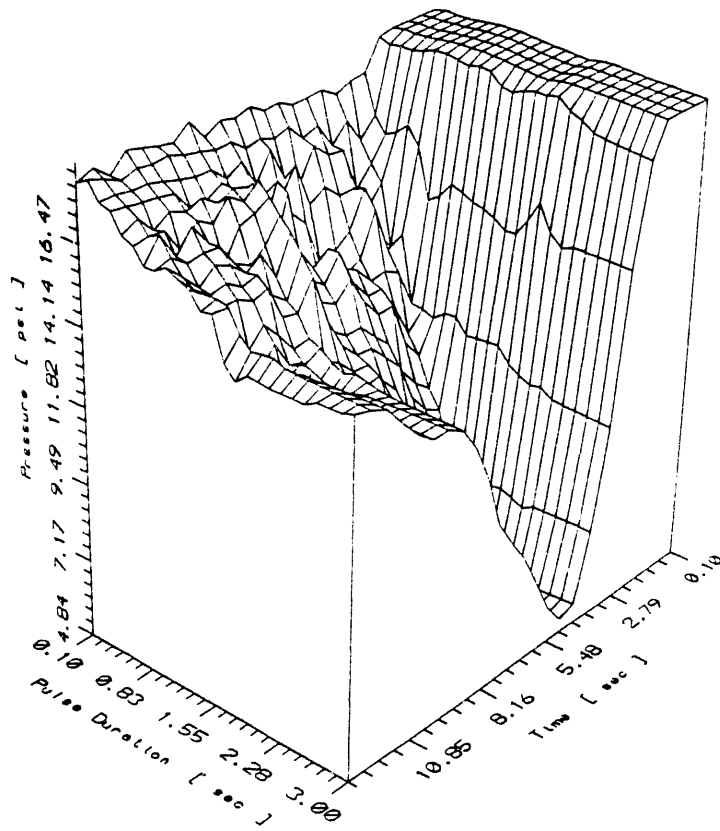


Figure 2. Nitrogen pressure variation ($p_{initial} = 18$ psi).

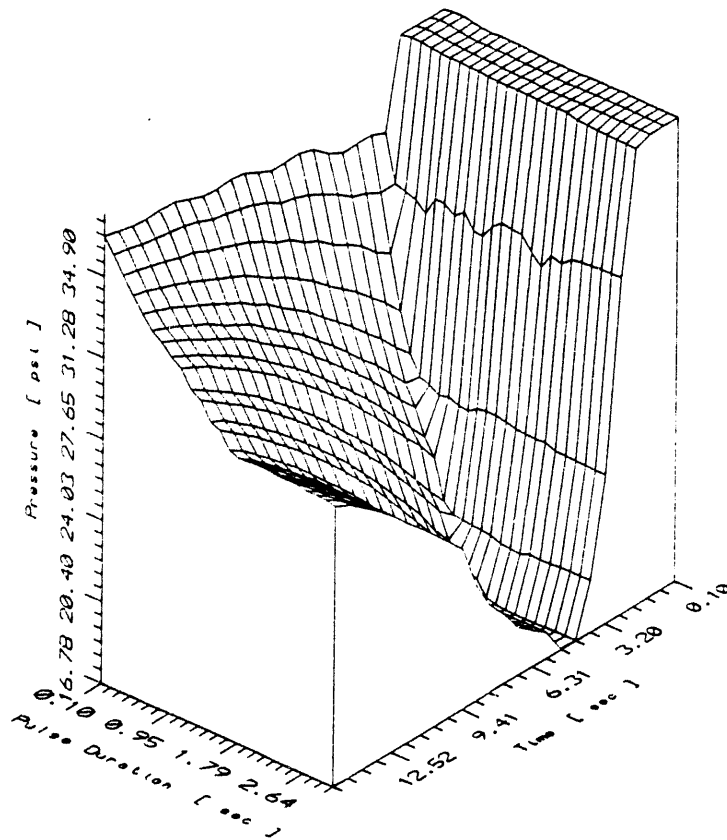


Figure 3. Nitrogen pressure variation ($p_{initial} = 37$ psi).

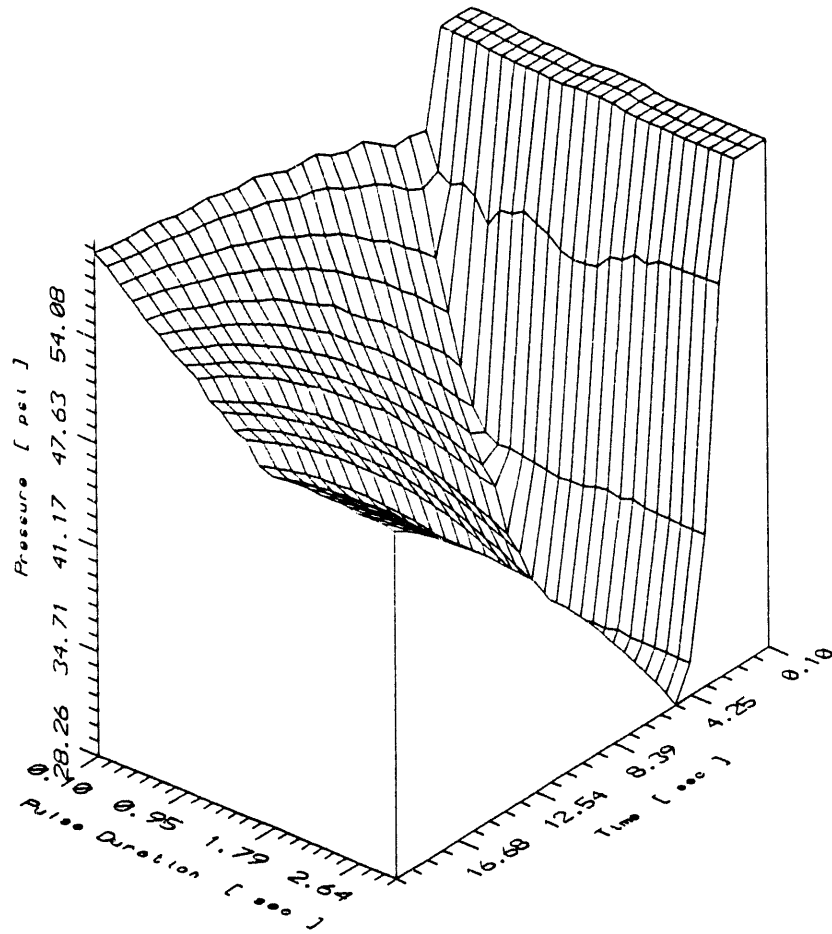
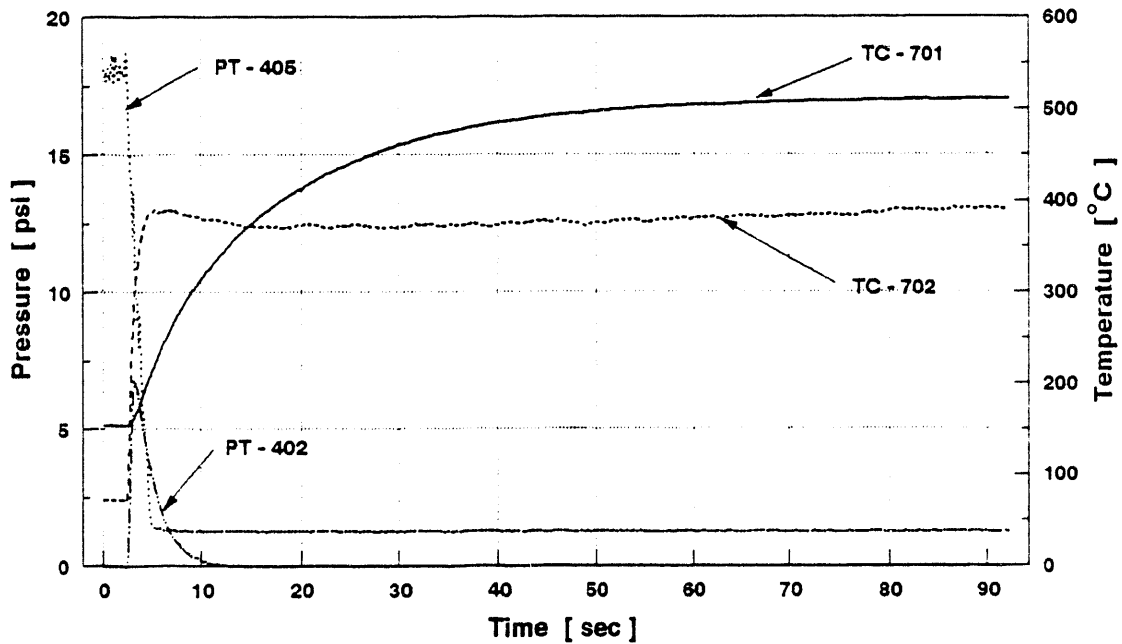


Figure 4. Nitrogen pressure variation ($p_{initial} = 60$ psi).

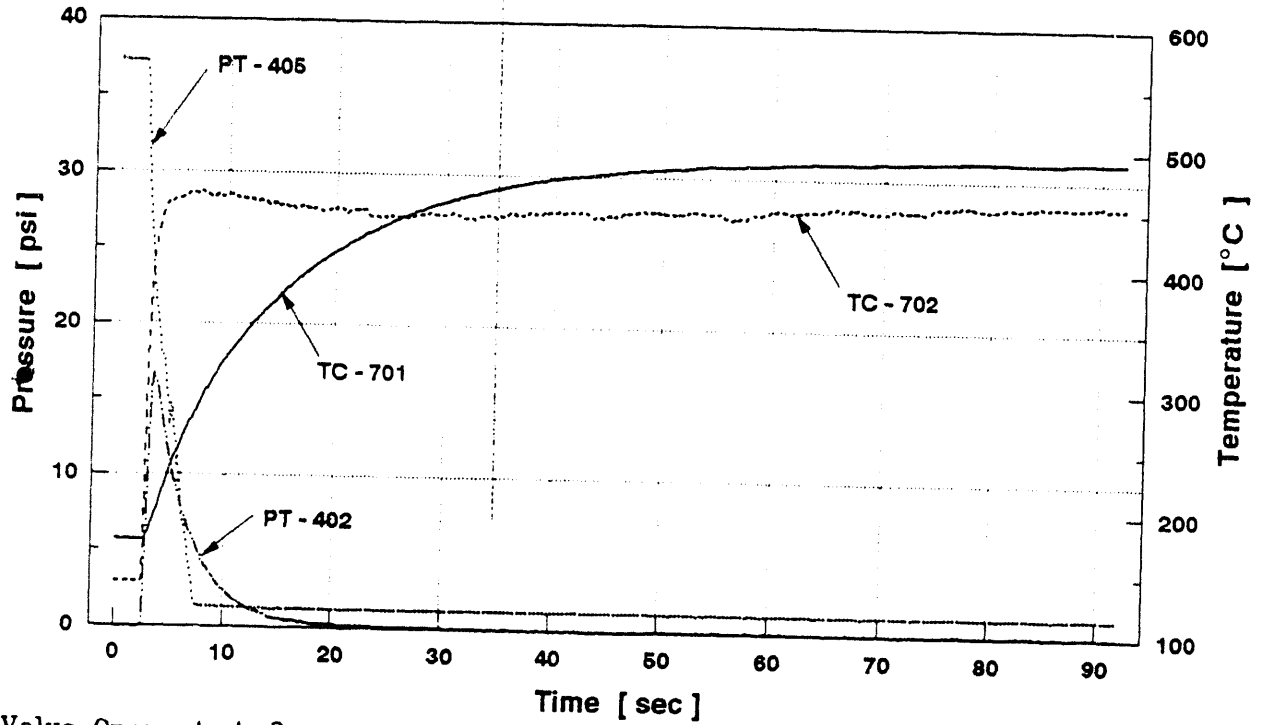
Infinite Pulse



Valve Open at $t=2$ sec

Figure 5. Infinite pulse ($p_{initial} = 18$ psi).

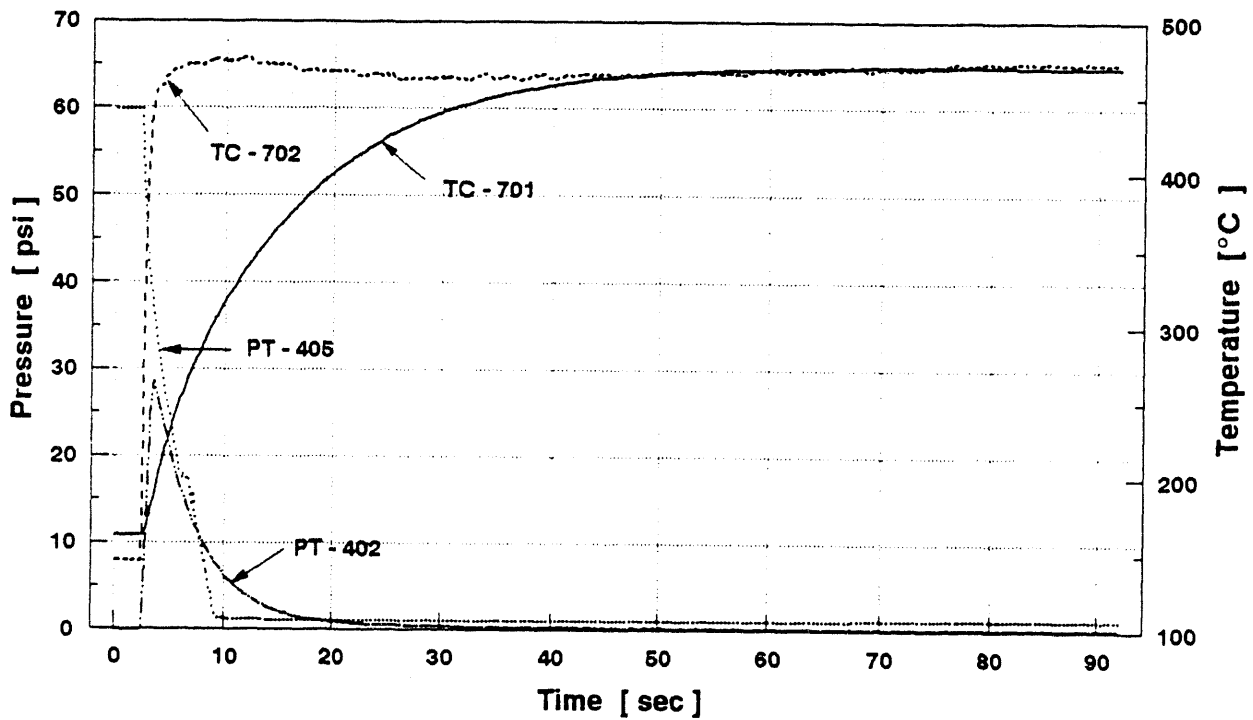
Infinite Pulse



Valve Open at $t = 2$ sec

Figure 6. Infinite pulse ($p_{initial} = 37$ psi).

Infinite Pulse



Valve Open at $t = 2$ sec

Figure 7. Infinite pulse ($p_{initial} = 60$ psi).

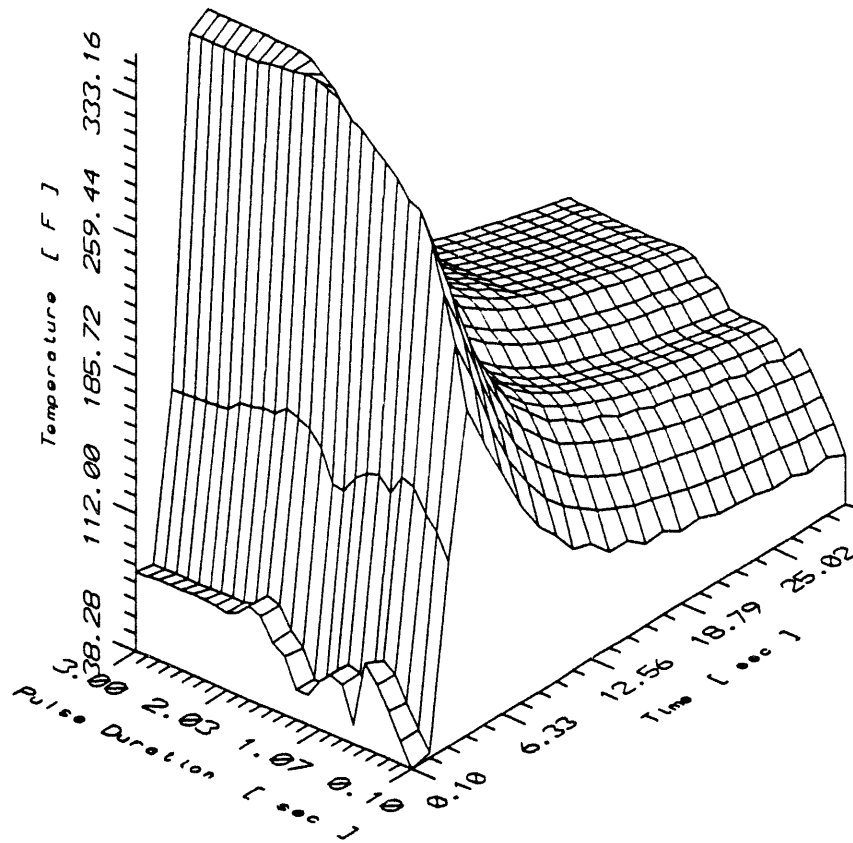


Figure 8. Backpulse gas temperature in front of the filter ($p_{initial} = 18$ psi).

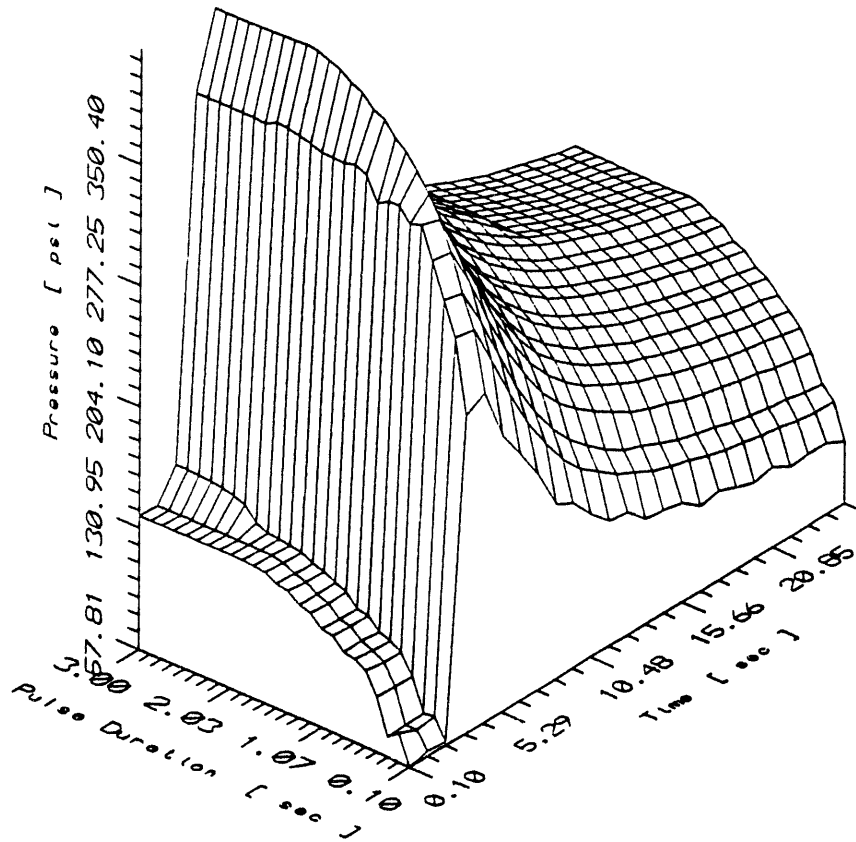


Figure 9. Backpulse gas temperature in front of the filter ($p_{initial} = 37$ psi).

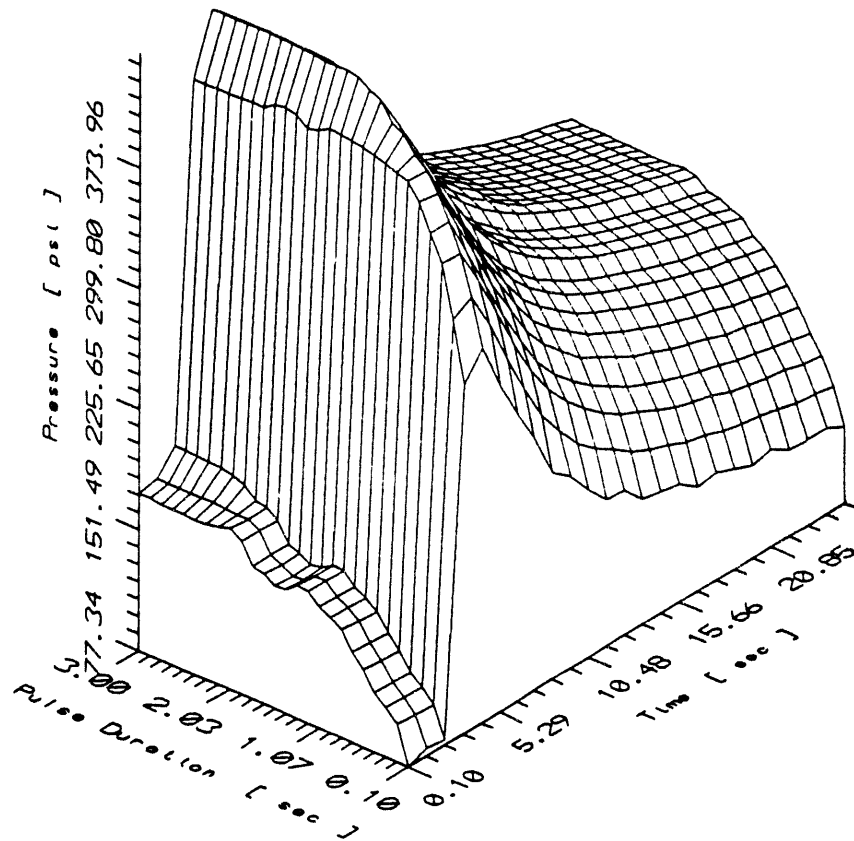


Figure 10. Backpulse gas temperature in front of the filter ($p_{\text{initial}} = 60$ psi).

Pressure wave intensity in front of the filter showed that both intensity and pulse duration are directly dependent on initial pressure level (see Figures 11 through 13). As expected, higher initial pressure resulted in a higher pressure wave intensity. The longer the solenoid valve was open, the longer the pulse duration that was involved.

A high-temperature, high-pressure, particle sampling system is being developed for use with the hot-gas cleanup test loop. This sampling system must meet the National Electrical Code (NEC) and B31.3 piping requirements as well as allowing sampling at the extreme operating conditions of the test loop. Aside from code-related issues, the particle sampling system currently in use is slow and cumbersome to use. A separate probe must be inserted to make flow measurements, then the particulate probe must be inserted to make dust-loading measurements. It takes approximately 45 to 60 minutes to collect one sample with the current configuration. While this system may be adequate for intermittent measurements on a temporary basis, it is inadequate for safe, reliable, long-term work. The particulate sampling system is being designed to sample at pressures up to 200 psi at a temperature of 1800°F under both oxidizing and reducing conditions. Table 1 shows the performance specifications for the sample system, and Figure 14 shows the sampling system. A sampling probe is inserted into the test loop, and a particulate sample is withdrawn isokinetically. The sample probe is considered to be disposable (based on wear). Different materials will be used for different operating conditions. The gas sample will pass through a series of cyclones and a borosilicate filter to remove all particulate matter, then through a quench train to remove any condensables, then through gas meters to determine flow. The probe and cyclone assembly will be electrically heated to maintain the gas temperature until it reaches the quench train.

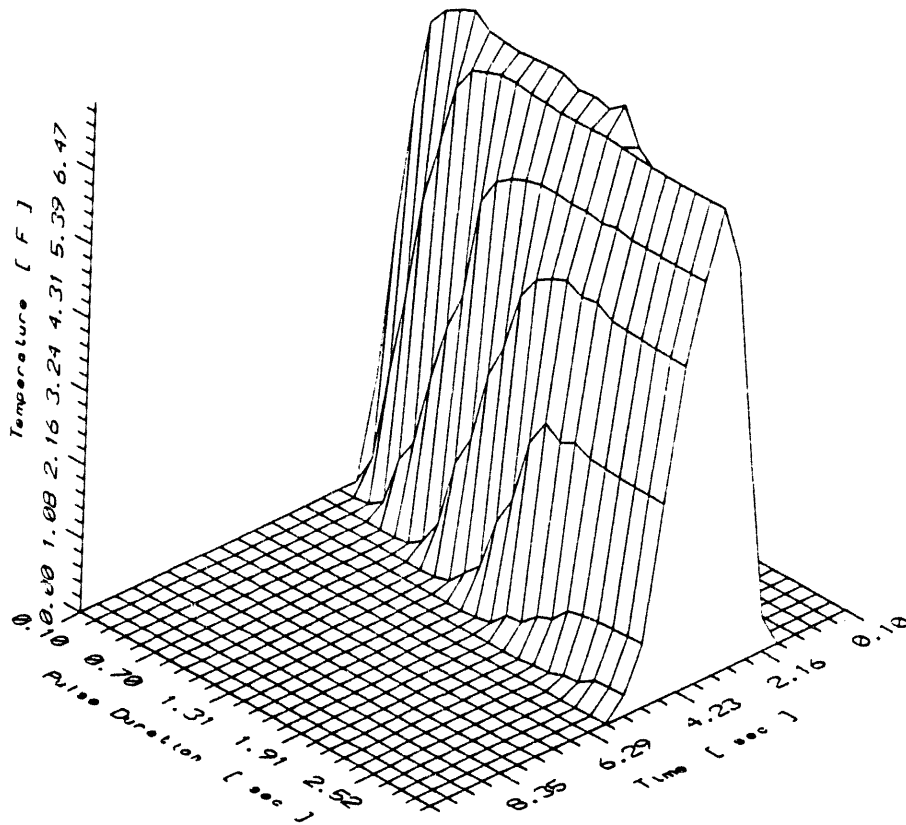


Figure 11. Pressure wave intensity in front of the filter ($p_{initial} = 18$ psi).

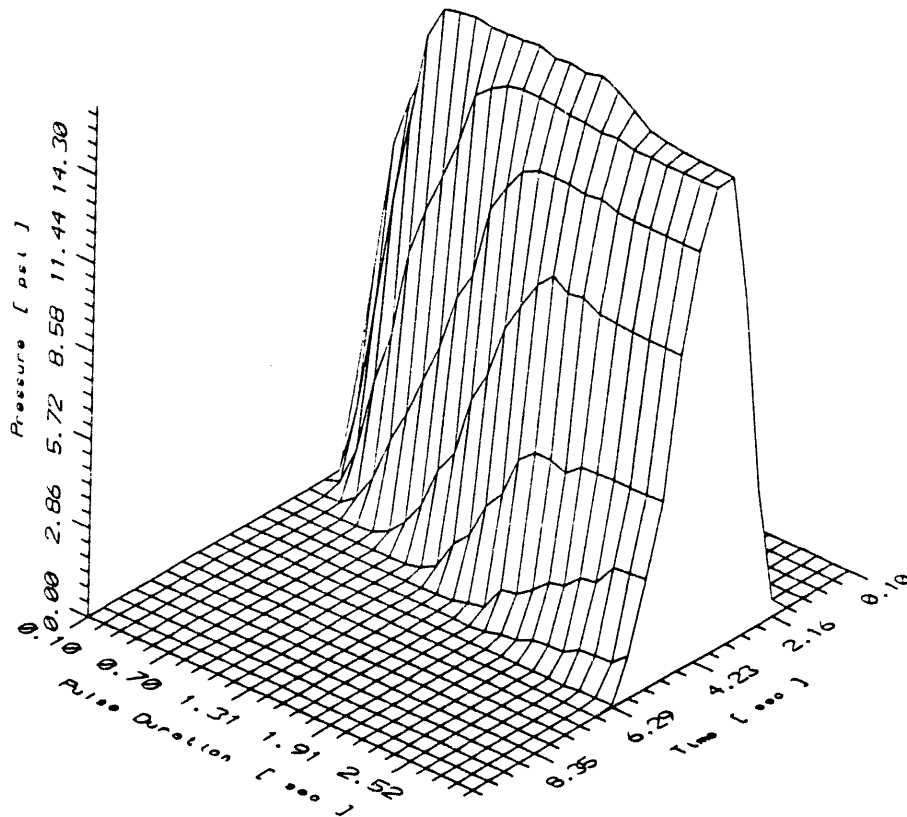


Figure 12. Pressure wave intensity in front of the filter ($p_{initial} = 37$ psi).

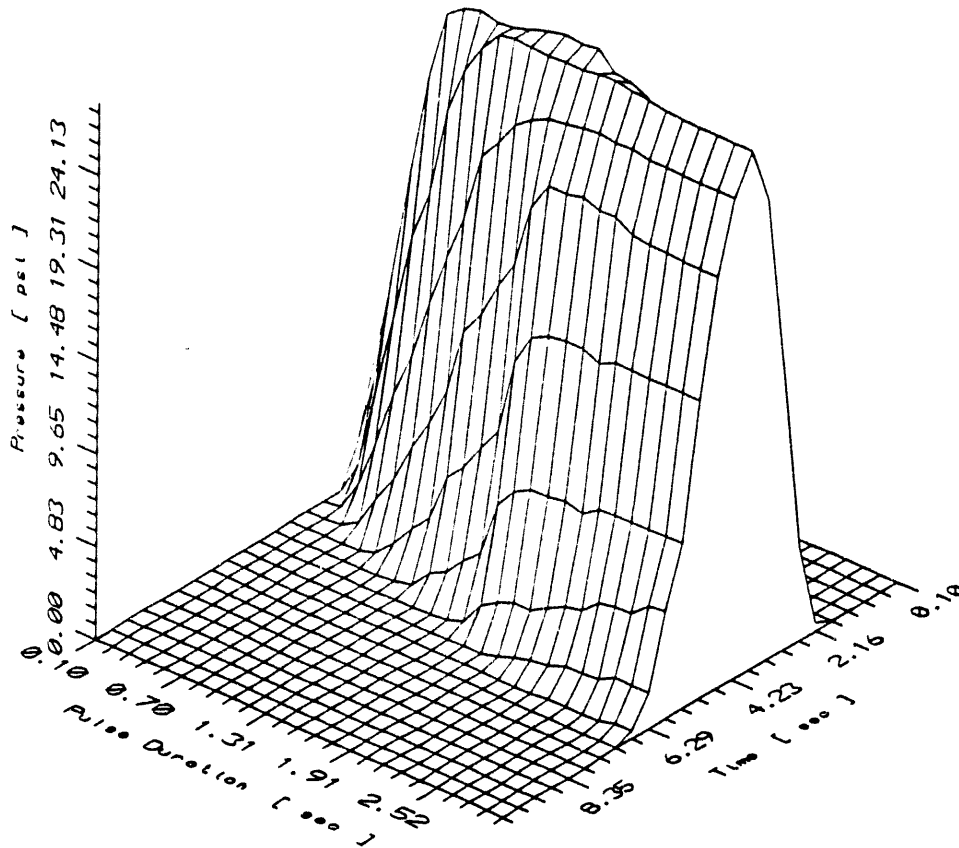
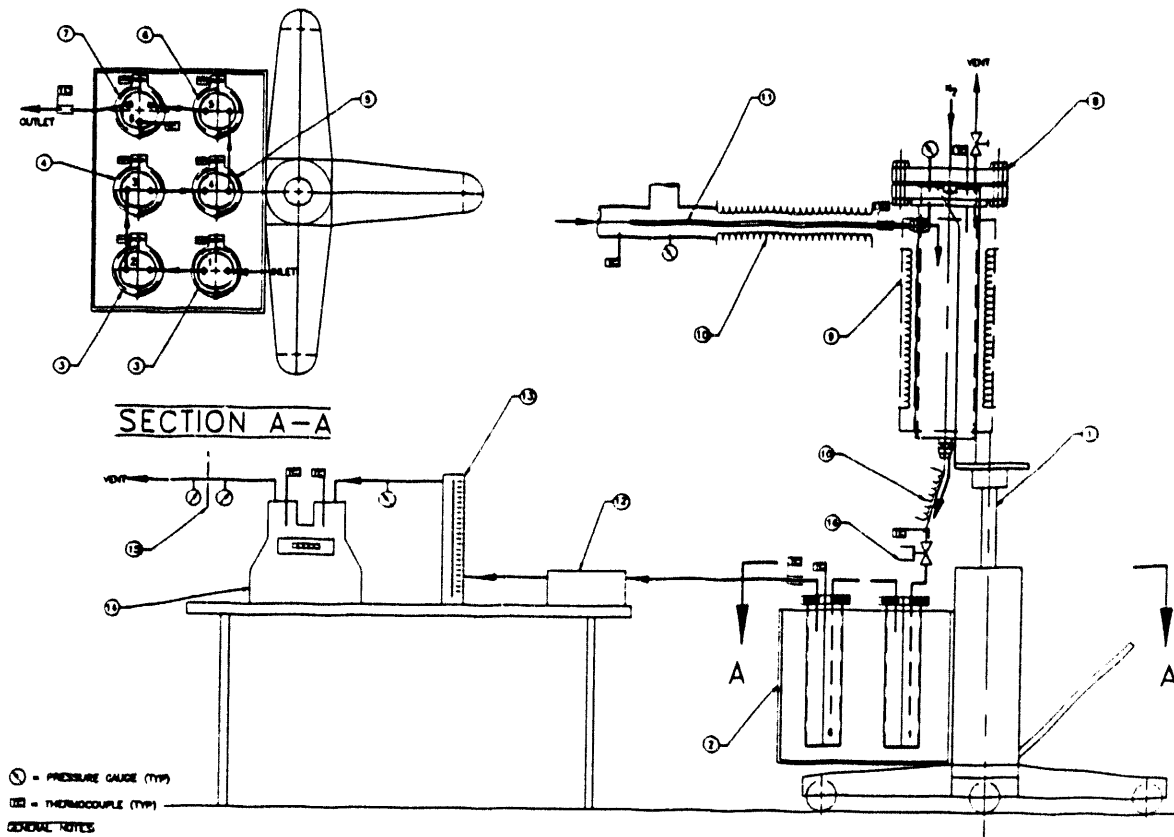


Figure 13. Pressure wave intensity in front of the filter ($p_{initial} = 60$ psi).

TABLE 1
Specifications for an Isokinetic Particulate Sampling System

Maximum Inlet Gas Temperature	1,800°F
Maximum Inlet Gas Pressure	200 psig
Gas Flow Range	2,000 - 30,000 scfh
Maximum Gas Temp. @ Filter	1,000°F
Typical Sample Rate	One Sample per Hour
Gases to be Sampled	Exhaust Gases from Coal Combustion and Gasification (Reducing and Oxidizing)
Electrical Classification (NFPA)	Class I, Div. 2, Group B
Applicable Codes	ASME B31.3 Piping Code



	17			
1	16		FLOW CONTROL VALVE	
1	15		ORIFICE METER	
1	14		DRY GAS METER	
1	13		FLOW METER	
1	12		OIL TRAP WITH INDICATOR	
1	11		SAMPLING PROBE ASSEMBLY	
2	10		HEAT TRACE LINE	
1	9		HEATER, SPLIT SHELL CERAMIC	
1	8		PARTICULATE SAMPLING ASSEMBLY	
1	7		ADSORBER, MOLECULAR SIEVE	
1	6		ADSORBER, ACTIVATED CARBON	
1	5		BUBBLER, SILICA GELL	
1	4		BUBBLER, DRY	
2	3		BUBBLER, SOLUTION	
1	2		GAS CONDITIONING TRAIN	
1	1		POSITIONING JACK, 2 STAGE PORTABLE	
QTY	ITEM	PART NO	DESCRIPTION	MATERIAL SPEC
ENERGY AND ENVIRONMENTAL RESEARCH CENTER				
GRAND FORKS, NORTH DAKOTA, U.S.A.				
PARTICULATE SAMPLER ASSEMBLY				
TOLERANCES UNLESS OTHERWISE SPECIFIED FRACTIONAL : 1/16 3 PLC. DEC. : 0.005 2 PLC. DEC. : 0.030 1 PLC. DEC. : 0.1 ANGULAR : 2-1/2 DEGREES		DRAWN BY: DMB		DATE: 1-10-92
		CHECKED BY: WRK		DATE: 1-14-92
		PROJ. MGR: GLS		DATE: 1-14-92
		APPROVED BY:		DATE:
		FINAL ASSY:		NEXT ASSY:
		FUND NO: 4358	WORK REQ: W1	SCALE: 1:4
		REV:	SHEET 1 OF 1	
				DWG NO: 1076

Figure 14. Particulate sampling system.

4.2 Pressurized Drop-Tube Furnace

Tests of kaolin as an entrained alkali getter in atmospheric and pressurized coal combustion systems were performed during this reporting period with the EERC pressurized drop-tube furnace system. Kaolin is a clay which is composed primarily of the mineral kaolinite ($\text{Al}_2\text{Si}_2\text{O}_5[\text{OH}]_4$). In pressurized fluid-bed combustion tests using granular filter beds, clays have been shown to be good sorbents for removing alkali compounds from the gas stream (1). In laboratory studies, kaolin has been shown to be effective not only at removing sodium compounds from the gas phase, but also in irreversibly fixing the sodium (2). Other clays are also believed to absorb sodium compounds from the furnace gas when the clay is added to the coal feed to a boiler. Emathlite has been shown to be especially good at getting sodium (2).

To be an effective getter, the clay material must not deposit once the sodium is fixed. This implies that the getting material must be composed of small particles, typically less than $5\ \mu\text{m}$ in diameter. Since clay particles normally have diameters smaller than this, they would appear to be ideal getting agents. However, moist clays can be highly agglomerated due to surface moisture, so it is best if the clay feed is dry before feeding to reduce agglomeration.

Kaolin was preferred for the getting test over other types of clays because it can be found in relatively pure form, containing less alkali and alkaline earth elements which may flux the material upon heating. Also, kaolinite has a layered structure composed of a sheet of silica tetrahedra bonded on one side to a sheet of aluminum hydroxide octahedra, so it has a higher aluminum-to-silicon ratio than most other clays. Because of its higher aluminum content, its possible fusion with an ash deposit will usually increase the viscosity of the deposit, thereby weakening it. Kaolin is mined in a number of places in the United States and can be supplied in rock, dried powder, or sieved dried powder forms.

Although a small body of data is available about the getters in laboratory experiments, limited data are available about the use of kaolin under carefully controlled coal combustion conditions, and none is available about its use in pressurized coal combustion conditions. Therefore, four tests were performed to test the efficacy of kaolin as a getter in both atmospheric and pressurized coal combustion conditions and to determine the mechanism of getting. The kaolin used for these tests was provided as rock by J.M. Huber Corporation of Macon, Georgia. It was dried, then ground in a mortar and pestle. Only fine powder was used for the getting experiments.

The kaolin powder was mixed with pulverized coal from the Spring Creek mine, Montana, in the ratio of 1 part kaolin to 2 parts ASTM coal ash. Spring Creek coal was chosen because it has relatively high sodium and low ash contents, and because the sodium is present in the coal as an ion associated with carboxylic acid groups in the organic structure of the coal. Because of this association, the sodium is vaporized during combustion. Vaporized sodium that encounters an ash particle is typically absorbed by the particle. However, Spring Creek coal produces little ash, so much of the sodium remains in the vapor phase in the hot zone of the combustor. In cooler regions of the boiler, it may condense homogeneously to ultimately form submicron sodium sulfate particles. There is some contention as to whether sodium hydroxide

condenses, then sulfates, or sodium sulfate directly condenses. In either case, at 1800°F, a considerable portion of the sodium is likely to be in the vapor phase. This sodium is very reactive and could cause severe corrosion of ceramic hot-gas particulate pollution control devices such as candle or cross-flow filters. Therefore, Spring Creek was chosen as a "worst-case" example of a coal that may cause alkali corrosion of ceramic hot-gas cleanup devices.

Four combustion tests were performed in all. One test each of raw Spring Creek at atmospheric pressure, coal plus kaolin at atmospheric, raw coal at 100 psi, and coal plus kaolin at 100 psi. The tests were performed in the EERC pressurized drop-tube furnace system (PDTF). The following description of the system is modified from that provided in the July through December 1991 semiannual technical progress report for the Turbine Combustion Phenomena project being performed under the Cooperative Agreement at the EERC.

The pressurized drop-tube furnace (PDTF) is capable of operating under the following conditions:

Temperature: ambient to 2732°F (1500°C)
Pressure: ambient to 300 psia (20.4 atm.)
Oxygen: 0-20 mol%
Gas Flow: 0 to 7.8 scfm (220 L/min)
Residence Time: 0 to 5.0 sec

- Optical access at any residence time
- Provision for char and ash collection
- Provision for ash deposition studies

A drawing of the PDTF facility is given in Figure 15. The entire PDTF is constructed of standard 24" and 6" flanged pipe sections. The large pressure vessel contains the electrically heated furnace sections of the PDTF as shown in Figure 16. Figure 17 is a photograph of the PDTF pressure vessel. The walls of the vessel are water-cooled to dissipate the heat from the furnaces. Optical access is provided by four 3" diameter ports in the pressure vessel. The optical sight ports are located below the secondary air preheater and top two furnace sections and above one furnace to reduce the temperature gradient across the optical access section. Electrical power is supplied to the furnaces through terminals in the bottom blind flange of the pressure vessel.

Above the large pressure vessel is the fuel injector section. The injector is a one-inch-diameter water-cooled probe sheathed in high-temperature insulation. Figure 18 is a photograph showing the translating mechanism used for raising and lowering the injector into the ceramic tube inside the furnace assembly. The injector may be retracted completely out of the furnace when not in use, or may be lowered into the furnace to give a residence time between zero and 5.0 seconds. Small viewports in the pipe crosses at the bottom and top of the injector section allow visual inspection of the probe and the sample-feeding behavior.

Below the large pressure vessel is a sampling probe assembly and translation mechanism. The construction details of the probe are shown in Figure 19. The sampling probe tip is interchangeable to allow ash deposit or fly ash samples to be collected without removing the entire sample probe. For the

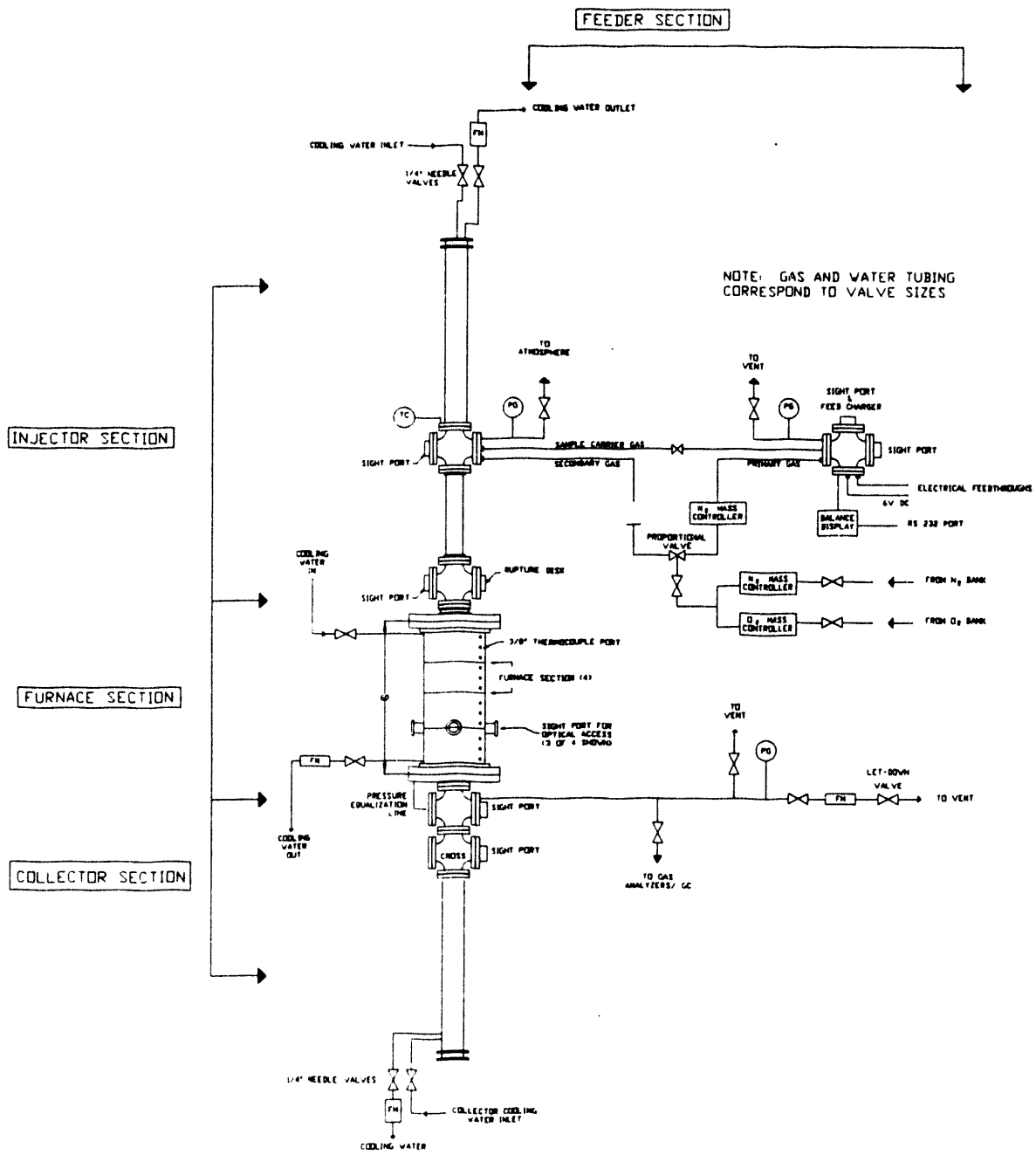


Figure 15. Pressurized drop-tube furnace process schematic.

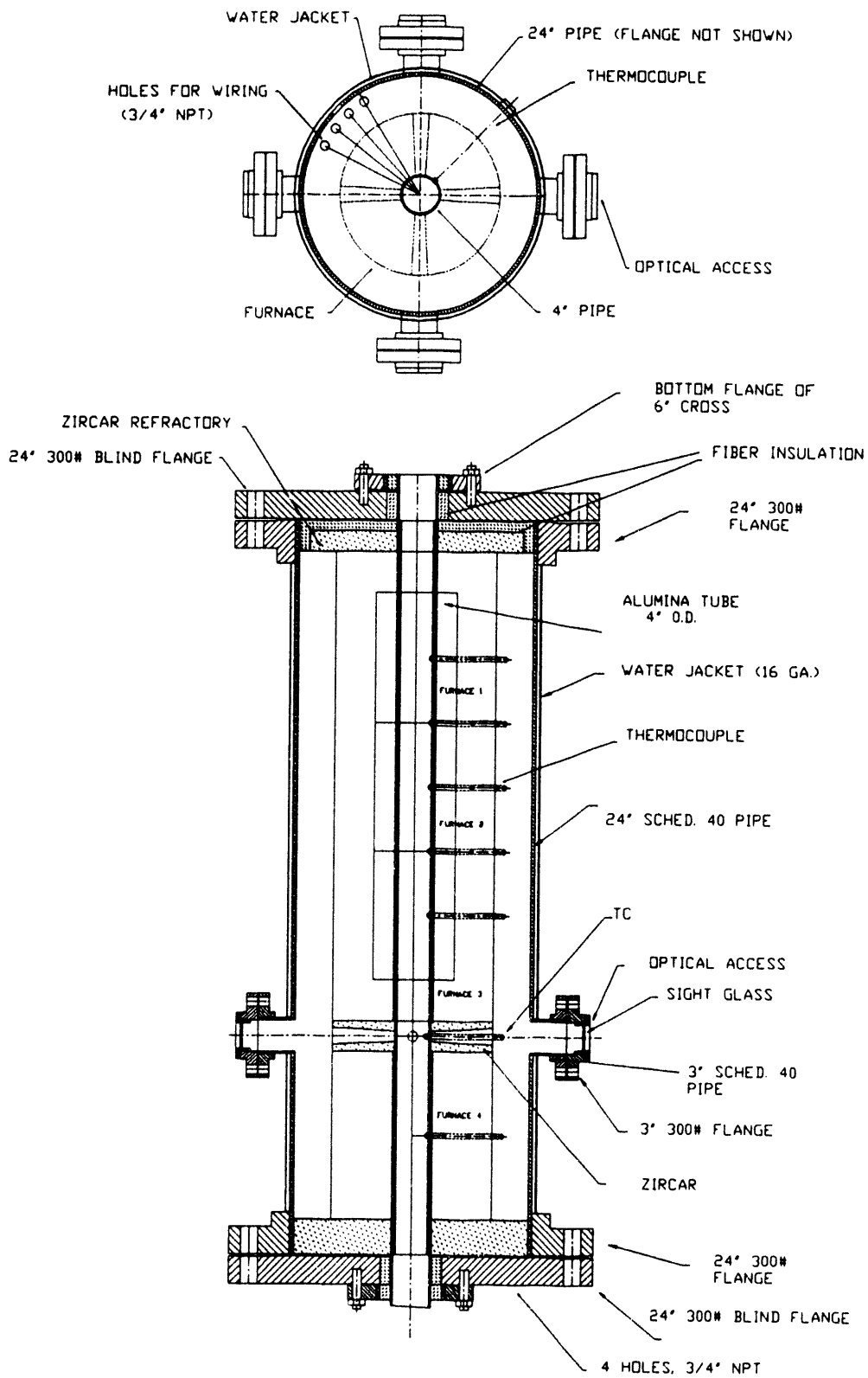


Figure 16. Furnace assembly in PDF vessel.

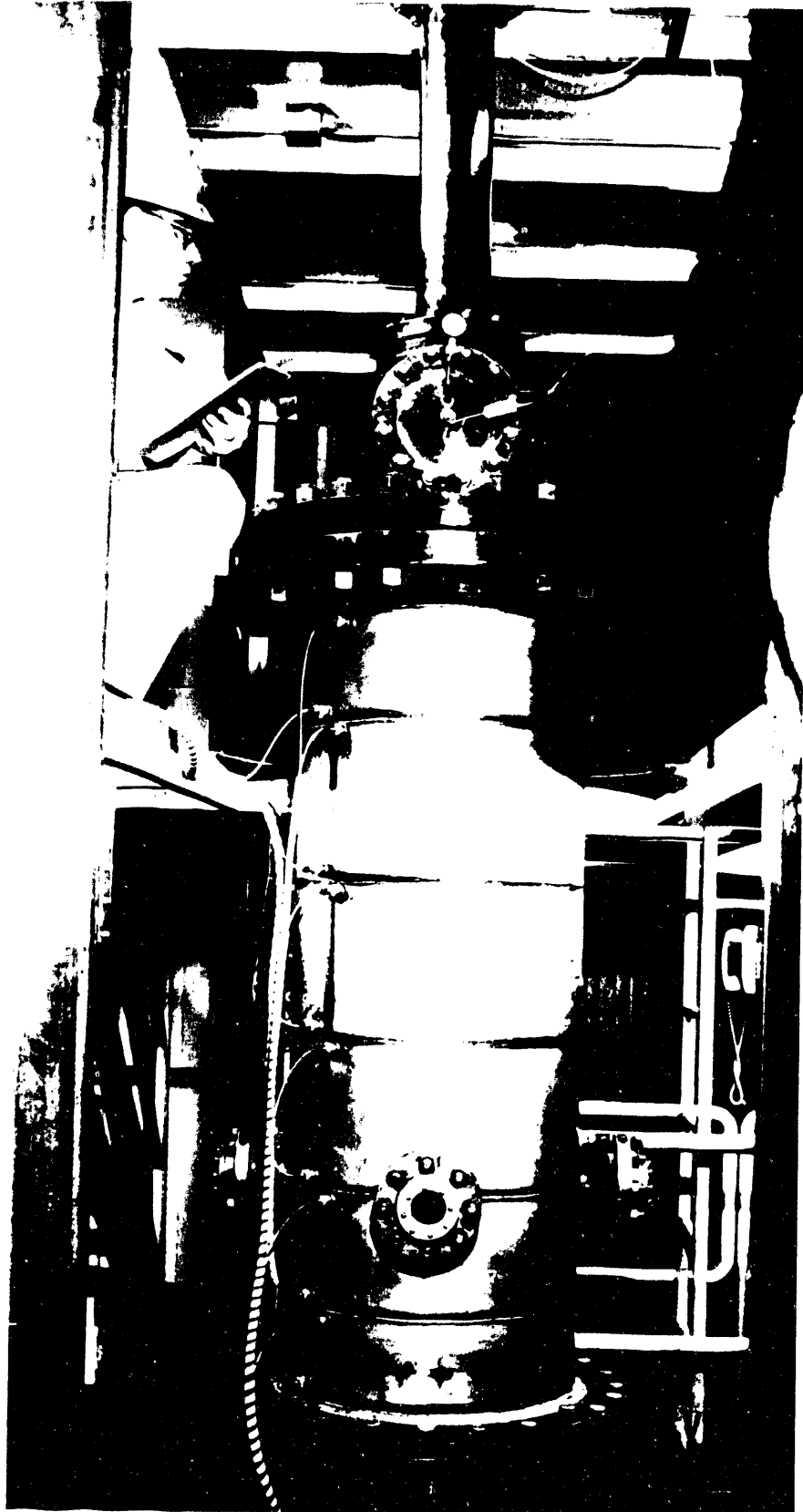


Figure 17. Photograph of PTFE pressure vessel.

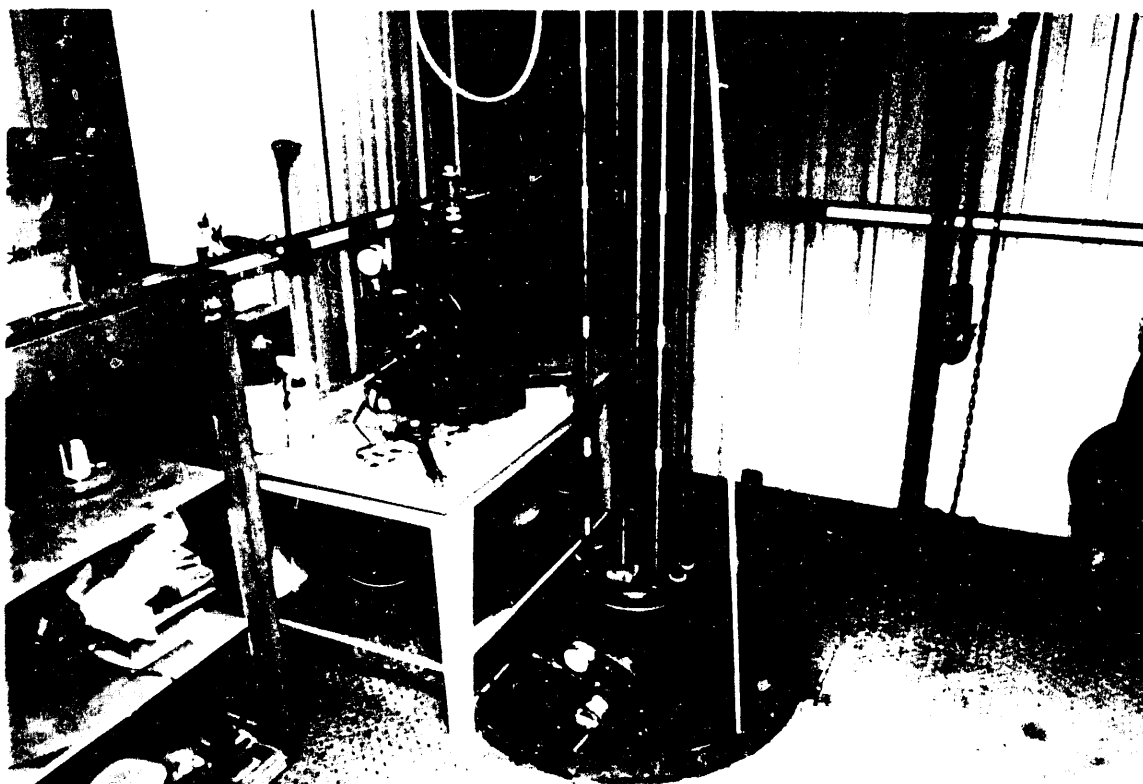


Figure 18. Photograph of PDTF translating mechanisms.

entrained getter tests, fly ash samples were collected and size-segregated on-line with a series of two cyclones and a final nylon filter. The sampling probe may be raised to the level of the optical access ports and retracted completely from the furnace for the removal of sample deposits or when not in use. Two pipe crosses with small sight ports allow inspection of the collection probe operation, and the removal of a blind flange provides access for the removal of sample deposits.

The sample feeder assembly is a blank flanged 6" pipe cross pressurized to slightly above the furnace pressure with gas connections to the furnace assembly. Figure 19 also shows the sample feeder pressure vessel located next to the sample injector translating mechanism. Figure 20 is a schematic of the coal feeder used in the PDTF. The design allows the actual sample feeder to be constructed of lightweight material, since it does not have to withstand more than slight pressure differentials. A small sight port allows inspection of the feeder operation, and the removal of a blind flange gives access to the vessel for filling or adjustment of the feeder. The lightweight feeder can then hang from a load cell in the pressure vessel to provide a continuous record of the sample feed rates. The gas composition and flow rate of gas into the PDTF is controlled by oxygen and nitrogen mass flow controllers. Gas composition can be controlled between 0-20 mol% at flow rates up to 220 L/min. The furnace pressure is controlled by a letdown control valve at the exit of the furnace.

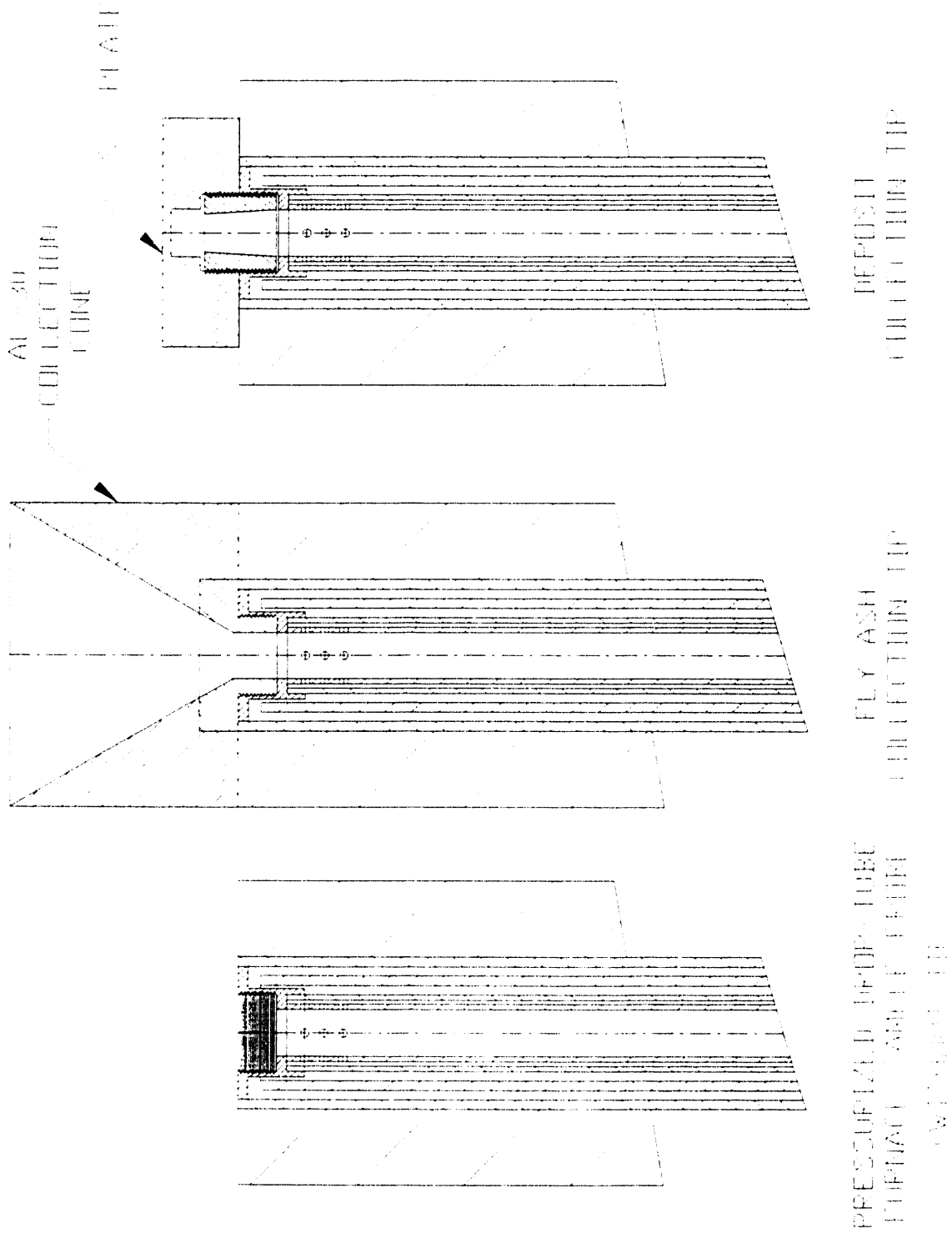


Figure 19. Schematic of PDFIF sampling probe with interchangeable tips.

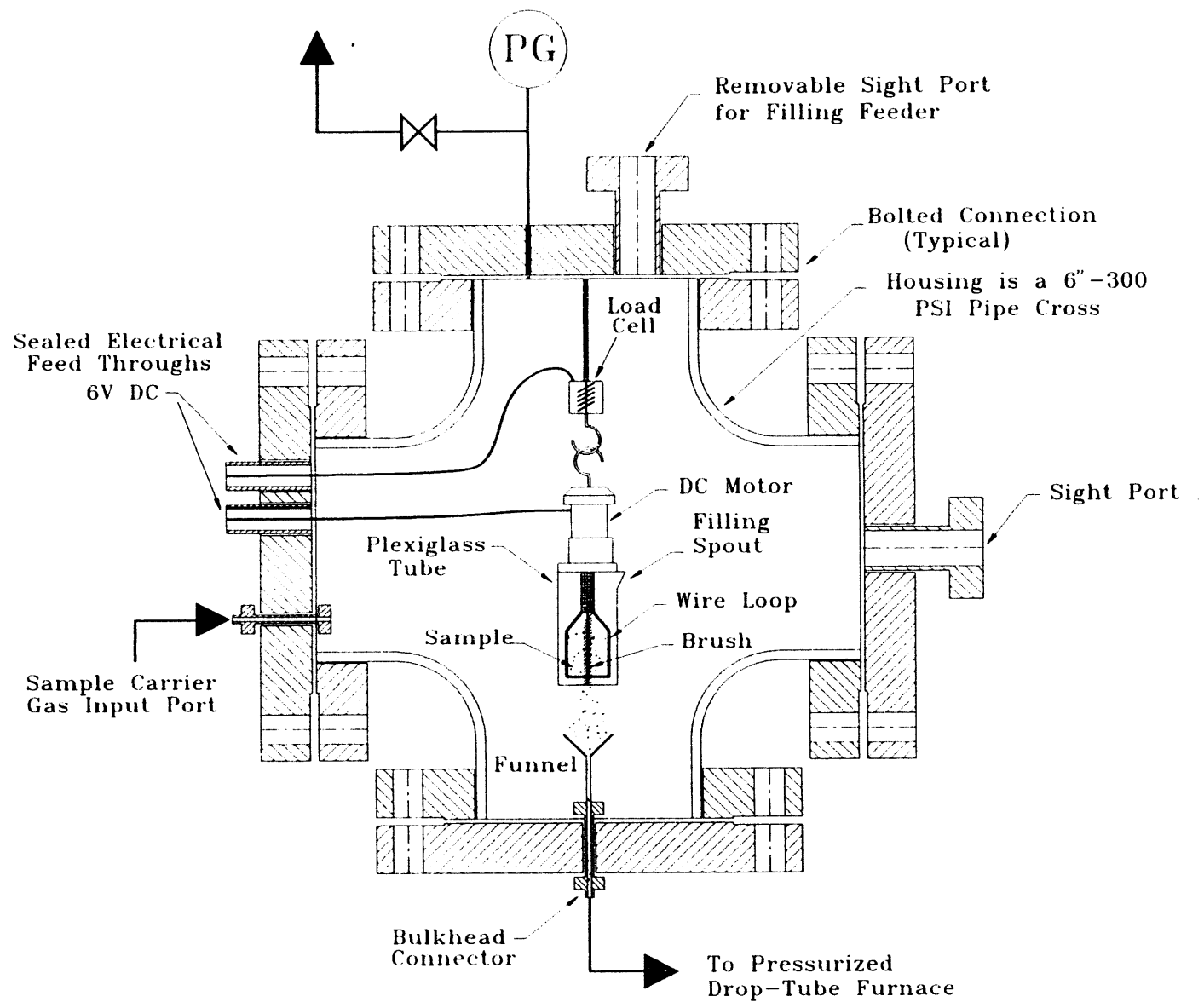


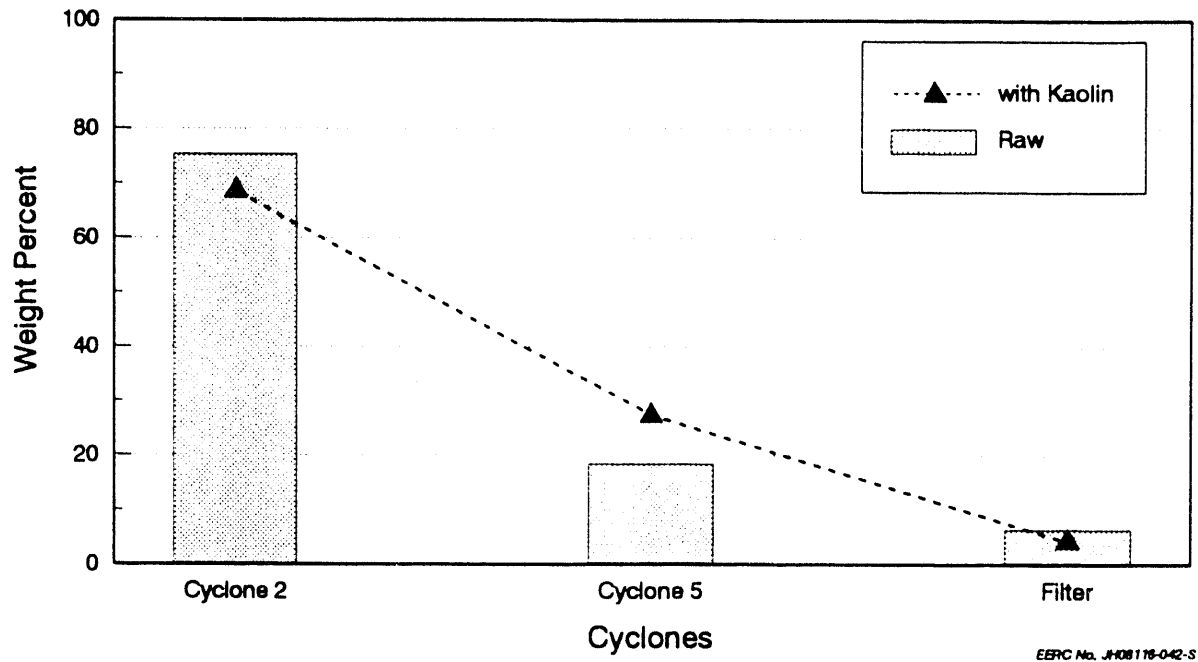
Figure 20. Schematic of coal feeder for pressurized drop-tube furnace.

Average PDTF conditions during the four alkali gettering tests are shown in Table 2. The excess air for the test of the raw Spring Creek coal at atmospheric averaged a negative 25%, indicating a fuel-rich condition for those tests. This may affect the phases that would form as compared to those that would form under oxidizing conditions, but is not expected to affect the size distribution of the sodium-rich phases, so the measured gettering effect is believed to reflect the level that would have been measured if the test were run in fuel-lean conditions. The temperatures reported for the separate furnaces are the temperatures measured at the wall of the central alumina tube. Zone 1 is at the top of the furnace, Zone 4 at the bottom where the collection probe is placed. The lower temperatures measured in Zone 3, optical section, and Zone 4 during the pressurized runs are caused by air influx through cracks in the optical system from the relatively cool space between the furnace and the pressure shell. The lower temperatures may have reduced the amount of gettering that would have occurred at pressure if there had been no air influx.

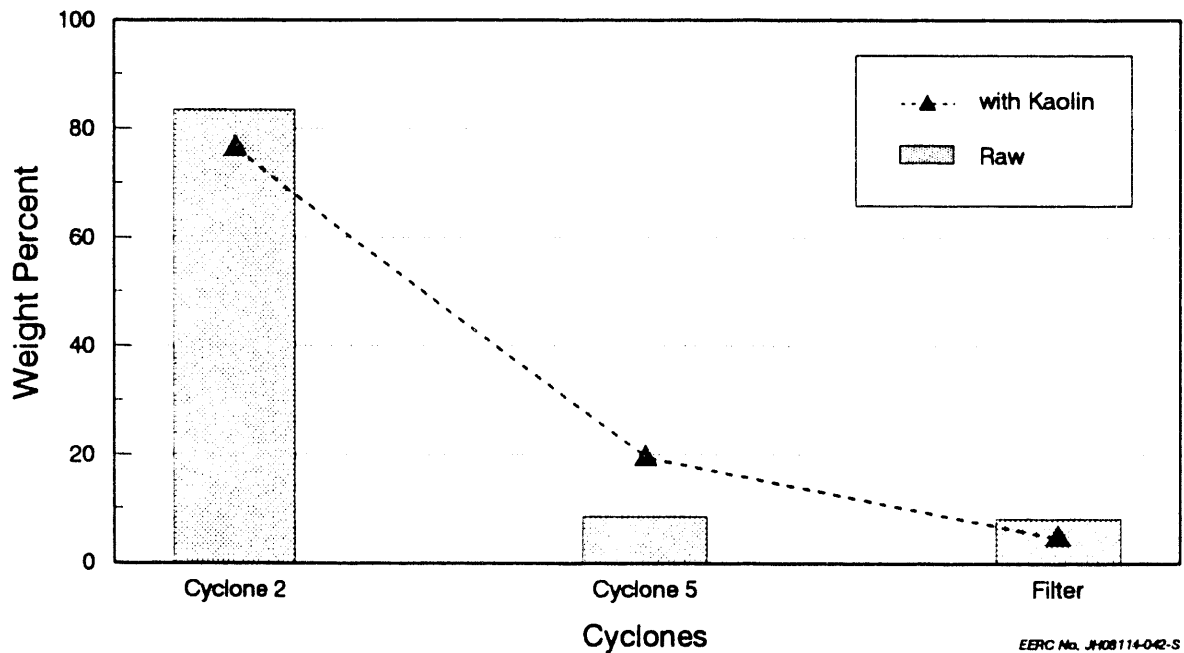
TABLE 2
Average Test Conditions for Alkali Gettering Tests
in the EERC Pressurized Drop-Tube Furnace System

	Raw Coal 2 psig	Coal+Kaol. 2 psig	Raw Coal 109 psig	Coal+Kaol. 109 psig
Feed Rate (g/min)	1.0	0.52	0.79	0.57
Excess Air (%)	-25	46	660	990
Zone 1 Tube T (°C)	1497	1497	1498	1498
Zone 2 Tube T (°C)	1497	1498	1494	1498
Zone 3 Tube T (°C)	1495	1496	1176	1212
Optical Zone T (°C)	1040	1061	921	1053
Zone 4 Tube T (°C)	1097	1097	903	981
Residence Time (s)	2.1	2.1	2.3	2.3

Figure 21 shows the percent of the total ash (corrected for unburned carbon) that was collected in each cyclone for each test. The bars represent the values for the raw coal tests, the lines represent the values for the test of the coal/kaolin blend. Because different flow rates were used for the atmospheric tests versus the pressurized tests, the cut points of the cyclones were different, so the data should not be used to determine changes in weight distributions due to pressure, only changes due to the addition of the kaolin. Attempts to measure the actual size distributions of the collected samples via laser light scattering (Malvern) were not completely successful because of particle agglomeration. In general, however, particles collected in Cyclone 2 (larger cyclone) had diameters greater than 10 microns; in Cyclone 5 (smaller cyclone) the diameters were between 1 and 10 microns; and on the filter they were less than one micron in diameter.



(a) Wt% of ash in each size fraction in the atmospheric pressure tests.



(b) Wt% of ash in each size fraction in the high-pressure tests.

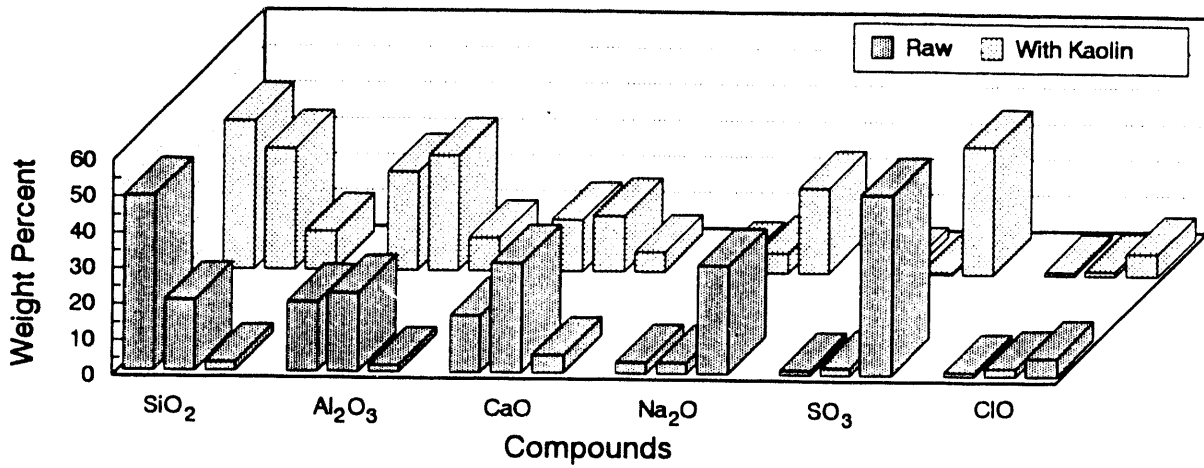
Figure 21. The percent of the total ash collected in each size fraction for the tests of kaolin as an alkali getter.

In both pressure and atmospheric tests of the raw Spring Creek coal, approximately 3/4 of the ash was collected in the larger cyclone with the remainder split over the smaller cyclone and filter. At both pressures a shift toward the middle (Cyclone 5) range of ash particles occurs when kaolin is added. The size shift occurs because the kaolin predominantly ends up in this size range in the ash. The effects of the addition on ash composition are illustrated in Figure 22. The figure contains 2 three-dimensional bar graphs showing the major element compositions of each size fraction of ash for each of the four graphs. Figure 22a presents data for the atmospheric pressure tests, Figure 22b for the high-pressure tests. In each graph, the front row of data gives compositions of the raw coal samples, the back row for the coal plus kaolin tests. For each element (reported as an oxide) within each data set, the three bars represent the compositions of the larger cyclone, smaller cyclone, and filter samples respectively moving from left to right. Other elements were either present in quantities of less than 5% or did not show any gettering behavior.

Figure 22 indicates only minor changes in ash composition versus size due to pressure differences. Because different size ranges were collected in the cyclones at different pressures, the influence of pressure on these changes cannot be determined unambiguously. However, all size-related variations are maintained when pressure is changed. As is true with most U.S. low-rank coals, silica is more concentrated in the largest size range than in the smaller ranges. The increases in silica and alumina contents in the Cyclone 2 and Cyclone 5 samples indicate that most of the kaolin that was added in the gettering tests ended up in those size ranges, primarily in Cyclone 5 as indicated by the size distribution data given in Figure 21. Unlike silica and alumina, elements such as sodium and sulfur that vaporize at some point during combustion tend to concentrate in the smallest size range. XRD indicates that sodium sulfate is the major crystalline constituent of this range. Much of the sodium sulfate likely formed through cooling during sample collection, either through homogeneous nucleation of sodium hydroxide which then sulfated, or by direct nucleation of the sodium sulfate. Because cooling rates are so rapid and no residual sodium hydroxide was indicated by XRD, the latter scenario is more probable.

To determine the efficacy of the kaolin additions in gettering, the weight distribution of elements among the different size ranges must be used. Figure 23 shows two combination bar-line graphs that illustrate the weight percent of the major elements that were collected for each test in each size fraction. Like Figures 21 and 22, two graphs are used, one for the pressurized tests, the other for the atmospheric tests. The bars represent the values for the raw coal tests, the lines represent the values for the test of the coal/kaolin blend. For each element, the three data points are for the larger cyclone, the smaller cyclone, and the filter, moving from left to right.

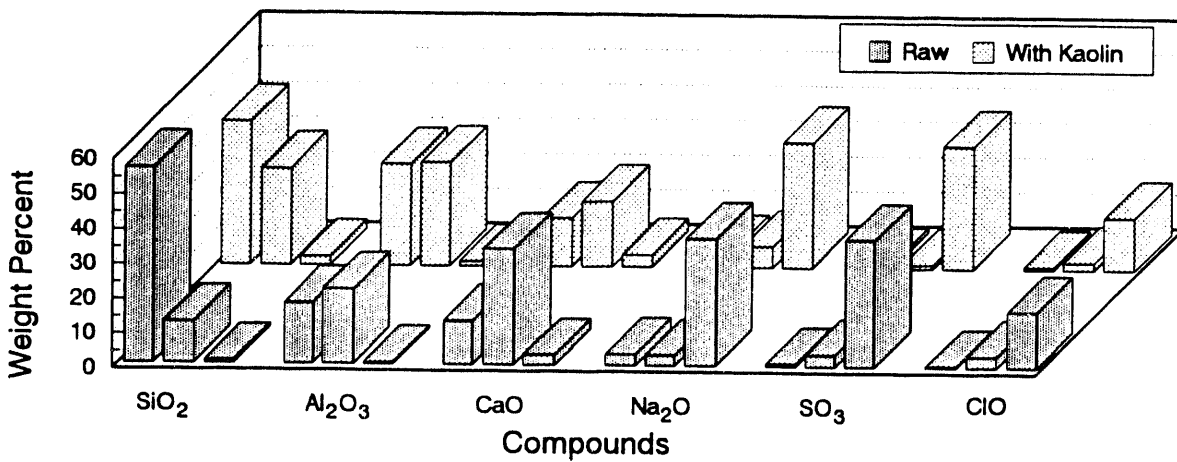
Silicon, aluminum, and calcium all tend to be predominantly concentrated in the larger particles, with negligible fractions present in the submicron particles. In contrast, large percentages of the sodium, sulfur, and chlorine are found in the smallest particles. Sulfur was bimodally distributed, most likely present as calcium sulfate in the largest particles and as sodium sulfate in the smallest particles. Because the cyclones had different size cut points for the atmospheric versus pressurized tests, the effects of pressure on the size distributions of the elements are somewhat ambiguous. It



Cluster order is Cyclone 2, Cyclone 5, filter.

EERC No. JH08135-042-S

(a) Major element composition of the ash in each size fraction in the atmospheric pressure tests.

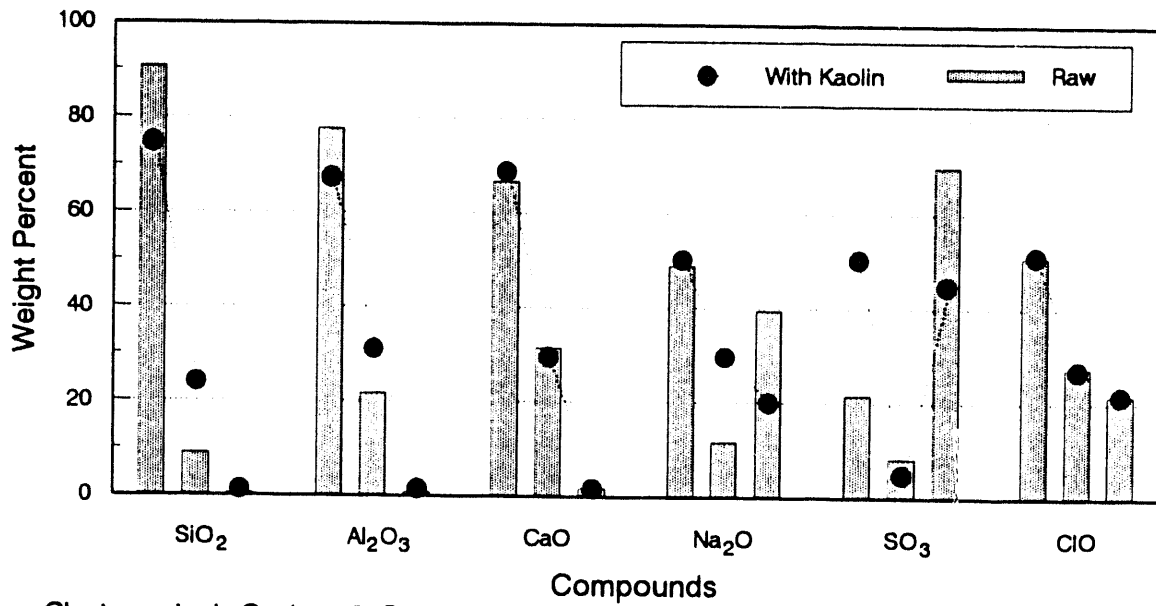


Cluster order is Cyclone 2, Cyclone 5, filter.

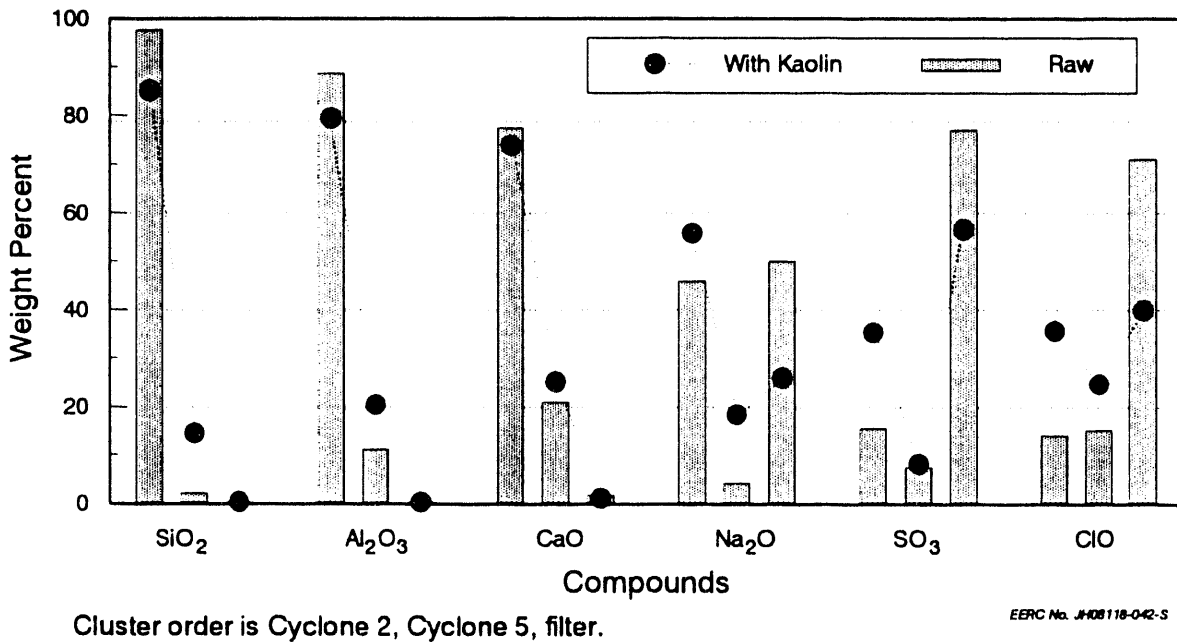
EERC No. JH08134-042-S

(b) Major element composition of the ash in each size fraction in the high-pressure tests.

Figure 22. The major element composition of the ash collected in each size fraction for the tests of kaolin as an alkali getter.



(a) Wt% of each element in each size fraction in the atmospheric pressure tests.



(b) Wt% of each element in each size fraction in the high-pressure tests.

Figure 23. The weight percent of each element collected in each size fraction for the tests of kaolin as an alkali getter.

is only clear that the weight distributions of all elements except chlorine among the different sizes are not strongly affected by pressure. In the raw coal tests, chlorine shows the only significant size shift, from larger to smaller particles at higher pressures. The chlorine-containing particles in the smallest size range probably formed during quenching of the gas during sample collection, indicating that at higher pressure more chlorine (probably as chloride) may exist in the gas phase than at atmospheric pressure. However, this conclusion is only preliminary at this point because there may have been some interference in the test data for chlorine.

The most important conclusion about the gettering tests is that sodium is shifted strongly away from the smallest particles by the addition of kaolin. If we assume that the sodium sulfate in the smallest size fraction formed when the gas was quenched during collection, then one half of the sodium was removed from the gas phase due to the kaolin addition. This result holds both at atmospheric and higher pressure. Most of the sodium was shifted to the 1- to 10-micron size range, which is where the kaolin is concentrated. The shift in sulfur from the smallest to the largest size ranges indicates that the sodium was chemically combined with the kaolin, probably in the high-temperature zone, and that the kaolin did not merely serve as a condensation surface for sodium sulfate. Because much of the sodium was removed from the gas phase, the sulfur shifted to the largest size range by sulfating additional quantities of the calcium-rich particles.

4.3 Thermochemical Equilibrium Modeling: PHOEBE Database Modifications

In the area of thermochemical equilibrium modeling, the following objectives had been set forth under Task D:

- 1a Improve PHOEBE database
- 2b Run simulations

Both items were addressed this fiscal year and are now complete. Item 1a, the improvements to the PHOEBE database, required a substantially (approximately 4 months) longer period of time than had been originally anticipated. However, the database now contains about 850 species, which is a threefold increase from its former size of about 270 species. Additionally, the database has also been thoroughly cross-checked. Validation tests have also been conducted and the database modified depending on the results of these tests. We also wish to emphasize that we expect the updating and validation process to be an ongoing activity throughout the lifetime of this (and possible other) projects.

The thermodynamic systems simulations of Item 2b have also been completed. Initially, very simple systems (like water, gas mixtures, etc.) with well-characterized thermodynamic behavior were simulated to validate the correctness of the overall PHOEBE algorithm as well as to optimize the standard free energy of formation values for many of the species in the database. A total of about 20 such simple systems were simulated. During this stage, the algorithm also underwent a few iterations of revisions and changes. Two real-life systems were selected for the final phase of this task item and their equilibrium behavior simulated. A comparison of the simulation results with the experimental phase diagrams shows quite acceptable results, the largest error in the simulated results being about 23%.

A list of chemical compounds relevant to advanced combustion systems was compiled. A variety of vapor and liquid-phase species were specifically chosen to better represent fluidized-bed combustion systems. The requisite free energy of formation (FEF) data for each species were also collated and entered into the database. The current PHOEBE database contains approximately 370 chemical compounds with an average of more than two physical phases (gas, liquid, or solid) per compound. This makes a total of roughly 800 species, which is a threefold increase over the original database. Appendix A is an index list of the database sorted by the names of the chemicals, and Appendix B is an index list of the database sorted by formulas.

The original PHOEBE database was modified to a Freeform ASCII database (FAD). This has the advantage that any conventional text-editing software can be used to edit the database. Also, since almost any text editor or word processor may be used to update, modify, or edit the database, specialized software to perform these tasks becomes redundant.

A database management utility that performs searching, retrieval, indexing, etc., was written (in C), debugged, tested, and is fully operational. Although these tasks can also be accomplished by some of the more advanced word processors, their specialized nature prohibits their execution by generic text editors.

Routines to curve-fit the free energy of formation data of the species have also been written. These routines allow a wide variety of representations (linear, polynomial, rational, logarithmic, etc.). The curve-fit representations of the FEF data can thus be chosen in the most optimal manner. In most cases, the curve-fitted FEF data are used, if need be, at the computation level.

4.3.1 Database Format Change

The advantages of FADs are twofold. First, since the database is simply an ASCII file, no specialized utilities are needed to maintain and manage the database, and the database can be transported to other operating systems or environments with no or minimal portability problems. Second, since data are entered in an arbitrary manner (with no fixed record or block size, etc.), adding, modifying, or updating entries in the database can be performed with any text editor or word processor. Once again, no specialized routines to perform these tasks are necessary. It may be noted that altering the record structure, which is quite complicated in the case of databases with fixed format records, is also trivially accomplished. Finally, since data for all of the fields of a record or chemical are often unavailable, the data entry process is also simplified to the extent that only available data need be input.

Thus each chemical in the PHOEBE database is viewed as a record, but without the limitations of fixed size and fixed number of fields. In turn, each record contains fields comprising two parts: a field identifier prefix (FIP) and the value for that field. Field identifier prefixes, as the name indicates, serve to identify the field for which the data are being entered. All FIPs start with the "dot" or "period" character (ASCII 0 H) and are followed by one or more alphabetic characters that are chosen to serve as acronyms for the field. For example, the FIP ".n" serves to identify the "name" field of the chemical, while the FIP ".f" serves to identify the

"formula" field of the chemical. Table 3 gives the list of FIPs and their explanations that are currently being used in the PHOEBE database.

TABLE 3
Field Identifier Prefixes (FIPs) and Explanations

<u>FIP</u>	<u>Explanation</u>
.n	Name of Chemical
.f	Formula of Chemical
.mp	Melting Point
.bp	Boiling Point
.p	Phase (Solid/Liquid/Gas) of Chemical
.r	Reference Citation for Data for Chemical
.v	Free Energy of Formation (FEF) Value(s) for Chemical
.end	End of Data for Chemical

As regards the value part of a field, the user simply enters the relevant data for a field subsequent to entering the FIP. For instance, for the FIP ".n" (the "name" field), the user will enter the chemical's name, while for the ".f" or "formula" field, the value part is the chemical's formula. A sample data entry for these two fields might look as follows:

```
.n Pyrite  
.f FeS2
```

Note that one or more spaces are mandatory between the FIP part and the value part of a field.

The FIP ".end" is a specialized prefix. It has no value part and is best thought of as not being an FIP at all. It is used to delineate the end of a record; that is, it is used to mark the end of data for each chemical. In principle, the use of such an "endmarker" is not necessary. However, the resulting algorithmic complexity in recognizing "end of record" without its use was sufficiently severe that it was deemed necessary.

To bring this discussion on the organization of the PHOEBE database into perspective, the actual data entry for aluminum has been extracted from the database and listed in Table 4.

4.3.2 Additions to Database

The original PHOEBE database contained approximately 130 chemicals (about 270 species) and was configured to analyze primarily the fly ash equilibrium behavior in pulverized coal- (PC) and cyclone-fired systems. However, a wide variety of condensed and vapor-phase species were not included due to lack of available data. Also, the emphasis was placed on condensed rather than vapor-phase components.

TABLE 4

PHOEBE Database: Record Entry for Aluminum

.n	Aluminum						
.f	Al						
.mp	933.25 ^a						
.bp	2793.0 ^a						
.p	s						
.r	Janaf						
.v	0.0 ^{b,c}	0.0	0.0	0.0	0.0	0.0	0.0
	0.760	1.878	2.951				
.p	ℓ						
.r	Janaf						
.v	7.180 ^{b,c}	6.053	4.926	3.798	2.671	1.535	0.384
.p	g						
.r	Janaf						
.v	288.816 ^{b,c}	275.243	261.785	248.444	235.219	222.112	209.126
	197.027	185.422	173.917	162.503	151.172	139.921	128.742

^a Melting and boiling points are in K.

^b FEF values are in kJ/mol and are in 100 K intervals starting at 300 K.

^c Not all the available FEF values are listed.

In contrast, PFBC and other advanced systems operate at elevated pressures, up to even 50 atmospheres, and it thus becomes necessary to analyze the probable phase and species distributions in these systems more critically. A simple case in point is the classic textbook example of the depression of the boiling point of water at elevated altitudes (lower atmospheric pressures) and its converse, the raising of the boiling point at higher pressures.

As a general rule, systems at elevated pressures exhibit critical behavior or phase transformations at higher temperatures as compared to systems at standard atmospheric pressure. The temperature ranges of condensed phases are thus usually prolonged, and melting is also usually skewed toward higher temperatures. Such considerations become especially important in regards to chemicals exhibiting thermal decomposition (carbonates, nitrates, hydroxides, etc.).

The selection of additional species to be included in the PHOEBE database was influenced by the higher operating pressures and the importance of alkali and reduced species in advanced systems. New species most relevant to these combustors were selected, and a literature search was conducted to collate the FEF and other data for these species. The primary sources of data references were Chase and others (3), Robie and others (4), Barin and Knacke (5), Hastie and others (6), and Kubaschewski and Alcock (7). The FEF data for an additional 240 chemicals have been now included in the database, so that the

current chemical count stands at 370 with about 800 species. This represents, approximately, a threefold increase in the size of the database.

In some cases, the FEF data over the entire range of 300 to 3000 K were unavailable. A variety of approximation and extrapolation techniques were adopted to ensure that data were available over the entire temperature range. It must be noted that the temperature range of 300 to 3000 K represents metastable regimes for almost all species (excluding perhaps some vapor-phase ones), and, hence, the requisite FEF data must usually be approximated.

The extrapolation technique used in many cases was that of graphical extrapolation wherein the formational free energy values are curve-fit to canonical or standard curves and the resulting curve extrapolated over the entire temperature range. In cases where the data were almost complete or almost linear, linear extrapolation was used to extend the range of the values. In the case of some vapor-phase species, however, since literature data were totally unavailable, the free energy values were computed from first principles as outlined in Mayer and Mayer (8) and McBride and Gordon (9).

In the case of a few liquids, data below the melting point were approximated by using a glass transition temperature ($\sim 7/10$ the melting point) and determining the free energy values by integrating the isobaric specific heat (C_p) data of the solid. It may be noted that the liquid may not necessarily cool to a glassy state in the metastable regime; nevertheless, as admonished by Chase and others (3), the use of a glass transition temperature is necessary to prevent an entropy paradox wherein the free energy of the thermodynamically more stable solid phase is higher than its metastable counterpart.

4.3.3 Database Utilities

A database search and sort utility and another utility to curve-fit the species FEF data have been implemented and are fully operational. As remarked earlier, these utilities are specific to the database and can be used to conduct a wide range of searches as well as select optimal curve fits for the FEF data.

The curve-fitting routines attempt to approximate the free energy data as a smooth function of temperature by regression. The basic ideas are as follows. Let μ° be the true FEF function and f_1, f_2, \dots, f_p a set of P -functions ("basis" functions). The approximate $\tilde{\mu}$ to the n FEF values is then defined by

$$\tilde{\mu} = \sum_{\alpha=1}^P c_{\alpha} f_{\alpha} \quad [\text{Eq. 1}]$$

where the coefficients c_1, \dots, c_p are determined by the condition that the residual R is defined by

$$\mathbf{R} = |\mu^o - \beta| = |\mu^o - \sum_{\alpha} c_{\alpha} f_{\alpha}| \quad [\text{Eq. 2}]$$

be a minimum, where $\|x\|$ denotes the norm of x .

Conventionally, the norm in Eq. 2 is taken to be the ℓ_2 or Euclidean norm, which then leads to a multilinear regression problem. With other norms, such as the ℓ_1 or ℓ_{∞} norms, the problem becomes nonlinear, and nonlinear minimization algorithms (such as the Marquardt-Levenberg algorithm) need to be utilized. Since the PHOEBE curve-fit routines are general purpose routines, both the linear and nonlinear cases are handled without any difficulty.

As to the choice of the approximating functions f_1, \dots, f_p , it may be mentioned that three particular sets of approximants are prevalent in the literature. The first is the linear approximant

$$f_1 = 1, f_2 = T,$$

the second is the log-linear approximant

$$\begin{aligned} f_1 &= 1 \\ f_2 &= T \\ f_3 &= T \ln T \end{aligned}$$

and, finally, the third is the log-hyperbolic-cubic approximant

$$\begin{aligned} f_1 &= 1/T \\ f_2 &= 1 \\ f_3 &= T \\ f_4 &= T^2 \\ f_5 &= T^3 \\ f_6 &= T \ln T \end{aligned}$$

Of these three, the 6-term log-hyperbolic-cubic approximant appears to be emerging as the accepted standard.

The PHOEBE database search and sort routines have also been implemented as fairly general purpose utilities. These allow the user to search the database in a variety of ways including searching by chemical name, by formula, by melting and boiling points, and by phase. The Boolean operations AND, OR, and NOT can also be used in specifying search criteria so that chemicals and species can be located very efficiently. In addition, a rudimentary regular expression matching facility is also included, enabling the user to specify search criteria in terms of regular expressions as well.

Currently, three sort options are available to the user to sort the chemicals in the data. One of these, of course, is to sort by the names of the chemicals, the other is to sort by the formulas of the chemicals, and the third option is to sort by the number of elements comprising the chemicals. Additional sorting categories, such as sorting by molecular or formula weight, or sorting by melting point, etc., can be included, although, in contrast to the search utility, no provision has been made to permit a dynamic sort

specification facility. The index lists in Appendices A and B have been constructed using the PHOEBE database sort utility.

4.4 PHOEBE Algorithm Extensions

The modules to enable equilibrium computations to be performed under different system pressures have been completed and incorporated into PHOEBE. These modules are, technically, "supervisory" modules in that the equilibrium behavior of the system under different system pressures is computed based upon user-specified or user-selectable models for the equation of state of the system. Thus a wide variety of equations of state, empirical and theoretical, can be simulated and tested, allowing for the possibility of optimal equations of state. The debugging and testing of these modules have been completed.

The entire set of PHOEBE routines, originally written in FORTRAN, have been rewritten in C to extend the portability of the package as well as to take advantage of the emerging object-oriented languages (such as C++). The overall algorithm has also been debugged and tested, and Section 4.4 describes some of the results obtained.

A preprocessor module has also been added to PHOEBE that allows the user to specify and work with thermodynamic systems in a fairly abstract manner. A given system once defined will be usable as a system in and of itself, or as part of a larger system. Some of the more common systems, such as "air," "xrf," "ultimate," etc., have been predefined and may be used as such. Thus, starting with simple systems, a whole hierarchy of systems can be defined leading to more complex systems such as coal blends, systems with additives, and so on.

Three major modifications have been carried out at the algorithmic level. The entire set of PHOEBE routines has been rewritten in C, modules to handle variations in system pressure have been incorporated, and an input data preprocessor has been added that permits abstract system definition and usage. Sections 4.3.2 and 4.3.3 describe, respectively, these modifications.

4.4.1 Original Algorithm Description

The original PHOEBE routines had been coded in FORTRAN. A menu-driven I/O preprocessor, written in ASSEMBLER, served as the user interface to the PHOEBE kernel. Maintenance, updating, and portability issues had been raised even then, but, for lack of other alternatives, were set aside. With the current proliferation of and advancement in windowed operating systems, Graphical User Interfaces (GUIs), and object-oriented languages, portability issues have become important. Thus one of the objectives of this task was the "modernization" of PHOEBE in terms of rewriting it in a more flexible and modern language.

The choice of C as the programming language was based on two reasons. One, the standardization of C is well in place, and a large number of operating system environments support the language so that the portability requirement is easily met. Two, interfacing with object-oriented languages, especially C++, is trivially accomplished, so that constructing friendly interfaces is also relatively simple. As mentioned earlier, the PHOEBE routines have been rewritten in C and a majority of them tested and debugged

during the coding stage itself. The overall program also has been tested for algorithmic correctness.

The central computational module in PHOEBE is an optimization routine that minimizes the Gibbs Free Energy of the system of interest. This minimization is achieved by varying the amounts of the species in the various phases until the smallest possible value of the free energy is achieved. More precisely, if the system comprises k phases whose free energies are G^1, G^2, \dots, G^k , the free energy G of the entire system is approximated as:

$$G = \sum_{\alpha=1}^K G^{\alpha} \quad [\text{Eq. 3}]$$

Note that Eq. 3 is exact if there are no phase-phase interactions or if these interactions are negligible.

The individual phase free energies G^{α} are in turn given by

$$G^{\alpha} = \sum_{i=1}^{N^{\alpha}} (\mu_{oi}^{\alpha} + \ln a_i^{\alpha}) n_i^{\alpha} \quad [\text{Eq. 4}]$$

$a_i^{\alpha} =$

where N^{α} is the number of species in the phase, n_i^{α} is the (molar) amount of species i in the phase, μ_i^{α} is the (standard) FEF of species i , and a_i^{α} is the activity of i within phase α . The ideal approximation to G^{α} arises when the activities a_i^{α} are approximated by:

$$a_i^{\alpha} = \begin{cases} 1, & \text{when } \alpha \text{ is a pure condensed phase} \\ \frac{n_i^{\alpha}}{\sum_j n_j^{\alpha}}, & \text{when } \alpha \text{ is a solution phase} \\ \frac{P}{P_0} \left(\frac{N_i^{\alpha}}{\sum_j n_j^{\alpha}} \right), & \text{when } \alpha \text{ is a gas phase} \end{cases} \quad [\text{Eq. 5}]$$

where P and P_0 are, respectively, the system pressure and the standard pressure.

The species amount or abundance vector n_i^{α} is not completely arbitrary, but has to satisfy the so-called mass balance and nonnegativity constraints. The mass balance constraints are linear equalities connecting the elemental amounts b_1, b_2, \dots, b_M (where M is the number of elements in the system) and the n_i^{α} . These can be succinctly expressed as:

$$b_a = \sum_{\alpha=1}^{\kappa} \sum_{j=1}^{N^*} S_{\alpha,j}^* n_j^* \quad [\text{Eq. 6}]$$

where $S_{\alpha,j}^*$ is the stoichiometry coefficient of element a in species j in phase α . The nonnegativity constraints

$$n_j^* \geq 0, \alpha = 1, \dots, \kappa, j = 1, \dots, N^* \quad [\text{Eq. 7}]$$

are conventionally not regarded as explicit constraints, but treated implicitly in the minimization algorithm. A more detailed account of this and other related aspects can be found in Ramanathan and others (10,11) and the references contained therein.

4.4.2 Pressure Calculations

It may be recalled from classical thermodynamics that the Gibbs Free Energy G of a thermodynamic system is defined as:

$$G = H - TS$$

where H is the enthalpy, T the temperature, and S the entropy of the system. In general, G is a function of the temperature T, the pressure P, and the molar amounts n_i^* of the species. Since almost all of the data on the free energy of formation of substances are for a particular pressure (usually, the standard atmospheric pressure), extrapolation of this data is necessary in order to study the equilibrium behavior of systems at elevated pressures.

This extrapolation is based on the fact that the pressure derivative $\frac{\partial G}{\partial P}$ of the free energy is the volume V of the system:

$$\frac{\partial G}{\partial P} = V \quad [\text{Eq. 8}]$$

so that,

$$G(T,P) = \int_{P_0}^P V dP + G(T,P_0) \quad [\text{Eq. 9}]$$

Eq. 9 is the key expression that permits the computation of the free energy for different pressures P, once the value $G(T, P_0)$ is known at a particular pressure P_0 . In order to perform the integration in Eq. 9, an explicit expression of the volume in terms of pressure is needed. This is usually obtained from an equation of state, either empirical or theoretical, for the system.

A variety of state equations are available in the literature, starting with the Van der Waals equations of state for (real) gases, to the Murnaghan

model (12) for condensed phases. The Murnaghan model, in particular, is predicated on the assumption that the bulk modulus B is an affine function of the pressure; i.e.,

$$B(T,P) = B_0(T,P_0) + nP$$

where $B_0(T, P_0)$ is the bulk modulus at the standard pressure P_0 and n is the pressure coefficient (usually about 4). Since the bulk modulus is related to the pressure derivative of the volume through

$$\frac{1}{V} \frac{\partial V}{\partial P} = \frac{1}{B} = \frac{1}{B_0 + nP}$$

integration of the above equation yields

$$V(T,P) = V_0(T) \left(1 + \frac{nP}{B_0}\right)^{-\frac{1}{n}} \quad [\text{Eq. 10}]$$

which may then be used in performing the integration in Eq. 9.

As remarked earlier, the pressure module routines in PHOEBE are primarily supervisory and can accommodate any user-specified equation of state. Such a capability is almost a must if formational free energies are to be computed at different pressures for a plethora of chemical compounds ranging over the spectrum of solid, liquid, and gaseous phases. Although some of the more standard equations of state are already built into the system, it is expected that an expanded library of such state equations will become a standard feature in PHOEBE in the near future.

4.4.3 Preprocessor Utilities

A significant enhancement in the area of problem statement and formulation in PHOEBE is the addition of preprocessor utilities that allow abstract (thermodynamic) system definitions and usage. Complex systems can thus be analyzed quite easily and naturally, and, since the facility is a dynamic one, a library or database of systems can be predefined and used in a straightforward manner.

Conventionally, one of the primary inputs to PHOEBE, the abundance or amount vector, had been specified at the elemental level, or in some cases at the oxide level. Algorithmically, this is the form of input that is needed and accepted by PHOEBE. However, from an application standpoint, this input format is quite inconvenient and cumbersome in many cases. For instance, in order to analyze the effect of additives such as alkali getters on performance, the most natural statement of the problem will be to define a thermodynamic system whose "components" are the coal and the envisaged additive. Another example is the analysis of coal blends. In this case, the "components" are the coals to be blended. There are many instances where an extended definition of a "component" of a thermodynamic system simplifies and, in some cases, even clarifies the problem formulation.

To accommodate these cases, preprocessor utilities have been added to PHOEBE that ease the drudgery of data entry and enable the user to specify the problem in a very natural manner. These utilities work by constructing a hierarchical diagram or a system definition tree (SDT) that contains the information relating a system to its subsystems and ultimately down to the basic components: the elements. (In the terminology of tree-processing, the elements constitute the "leaves" or "external nodes" of the SDT). Note that the recursive definition of trees implies that SDTs can be imbedded to any arbitrary level, limited only, perhaps, by available memory. A typical SDT starts with the highest-level abstract specification and successively gets more and more concrete until finally the definitions reduce to lists of chemical formulas or elements. For instance, the following definition-set:

```

Fuel      = Air, Coal
Coal      = Ultimate, Ash
Ultimate  = H2O, CO2, SO2, NO2
Ash       = Al2O3, SiO2, MgO, CaO
Air       = N2, O2, CO2
  
```

is an example of an abstract thermodynamic system, "fuel," and illustrates the utility, flexibility, and power of abstract system definitions. The SDT of this system has as its root the node "fuel" with two principal branches, connecting the (sub) systems "air" and "coal." Figure 24 displays the SDT of this model system. In the figure, the elemental nodes or leaves of this tree are also displayed.

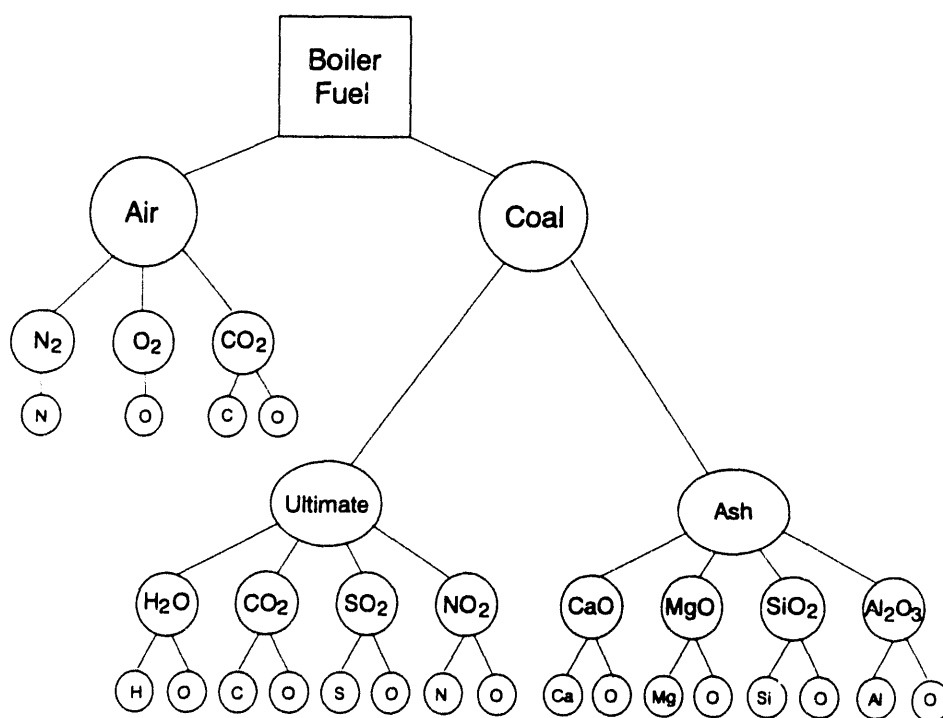
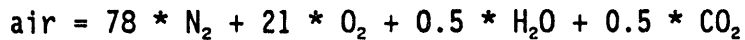


Figure 24. An example system definition tree (SDT).

In some cases it proves useful to define systems with a fixed stoichiometry between its subsystems. For example, the thermodynamic system "air" is commonly considered to be a system containing O₂, N₂, H₂O, and CO₂ in fixed proportions. To accommodate such fixed stoichiometry systems, a PHOEBE system definition tree is permitted to have an optional stoichiometry specification as well. Thus, for example, one can define the system "air" as:



so that the stoichiometry values (78, 21, etc.) become built into the definition of the "air" system.

4.4.4 Tests of the Database Algorithms

Two phase diagram calculations were performed with PHOEBE as part of overall program verification as well as to gain an understanding of the program's accuracy. In general, phase diagram calculations are very time intensive since the free energy of the system needs to be repeatedly minimized as the program steps through the extensive variables (like temperature and component amounts). The two phase diagram calculations that were done, for instance, took a total of 4 hours to compute (and plot). The results of these calculations are displayed in Figures 25 and 26.

Figure 25 is a plot of the experimental versus PHOEBE-predicted phase diagram for the binary system Al₂O₃ - SiO₂. (The solid lines are the experimentally determined phase boundaries while the dotted lines are the predicted phase boundaries.) Figure 26 is a plot of the experimental versus predicted phase diagram of the system Na₂SiO₄. (This represents a cross-section of the ternary system Na₂O - Al₂O₃ - SiO₂.) As can be seen from these figures, the predicted values track the experimental values fairly well with the largest error being about 23%. It should also be noted that both these systems were assumed to behave ideally (i.e., with unit-activity coefficients) so, necessarily, we expect errors in the predicted values since it is well known that these systems are nonideal. Additionally, it must also be borne in mind that inherent inaccuracies exist in the FEF values in the database. All in all, therefore, it can be concluded that PHOEBE provides acceptably accurate representations of the equilibrium behavior of multiphase, multicomponent systems.

5.0 FUTURE WORK

5.1 Particulate Control

Future work will consist of making modifications to the test loop to improve outlet particulate loading data, relocating some of the instrumentation, adding additional instrumentation, building the particulate sampling system, continued testing of filter elements, performance characterization of the heated backpulse system, and studying various alkali issues as they relate to advanced cycle power systems.

The design work required to relocate the test loop cannot be done until the location of the test loop is determined. This is contingent upon the size, shape, and location of the TRTU. For this reason, some of the design

$\text{Al}_2\text{O}_3\text{-SiO}_2$

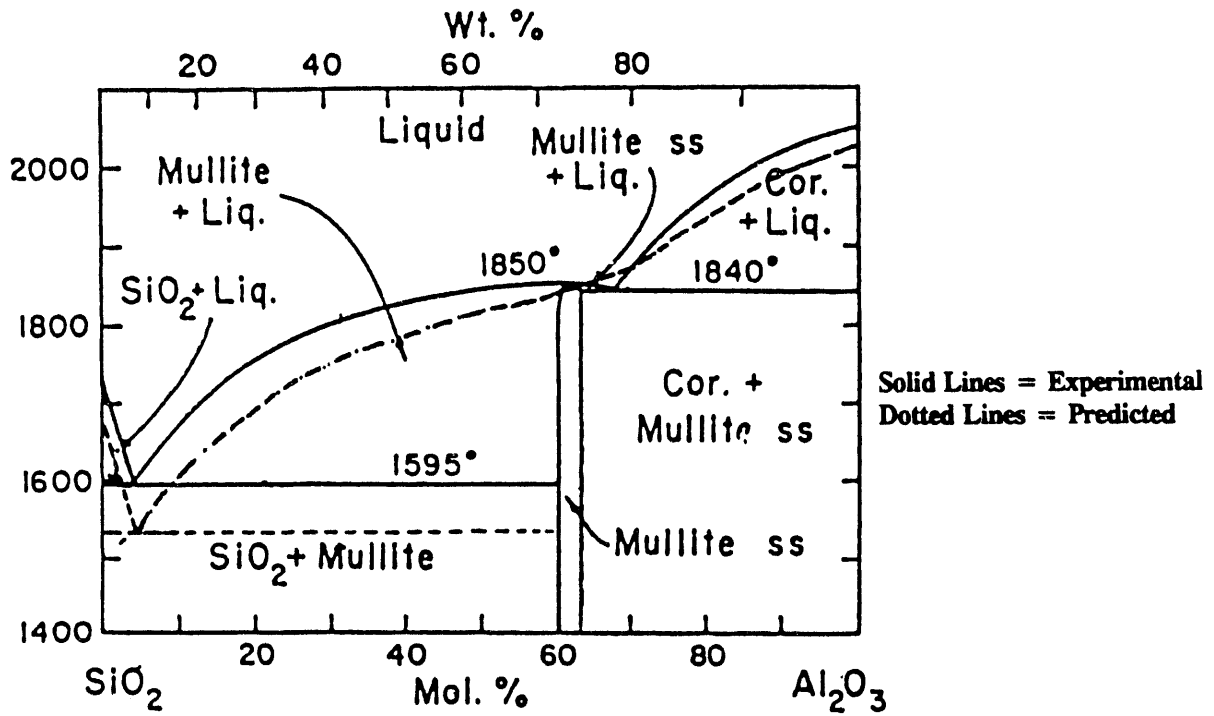


Figure 25. A plot of the experimental PHOEBE-predicted phase diagram for $\text{Al}_2\text{O}_3\text{-SiO}_2$.

$\text{Na}_2\text{O-Al}_2\text{O}_3\text{-SiO}_2$

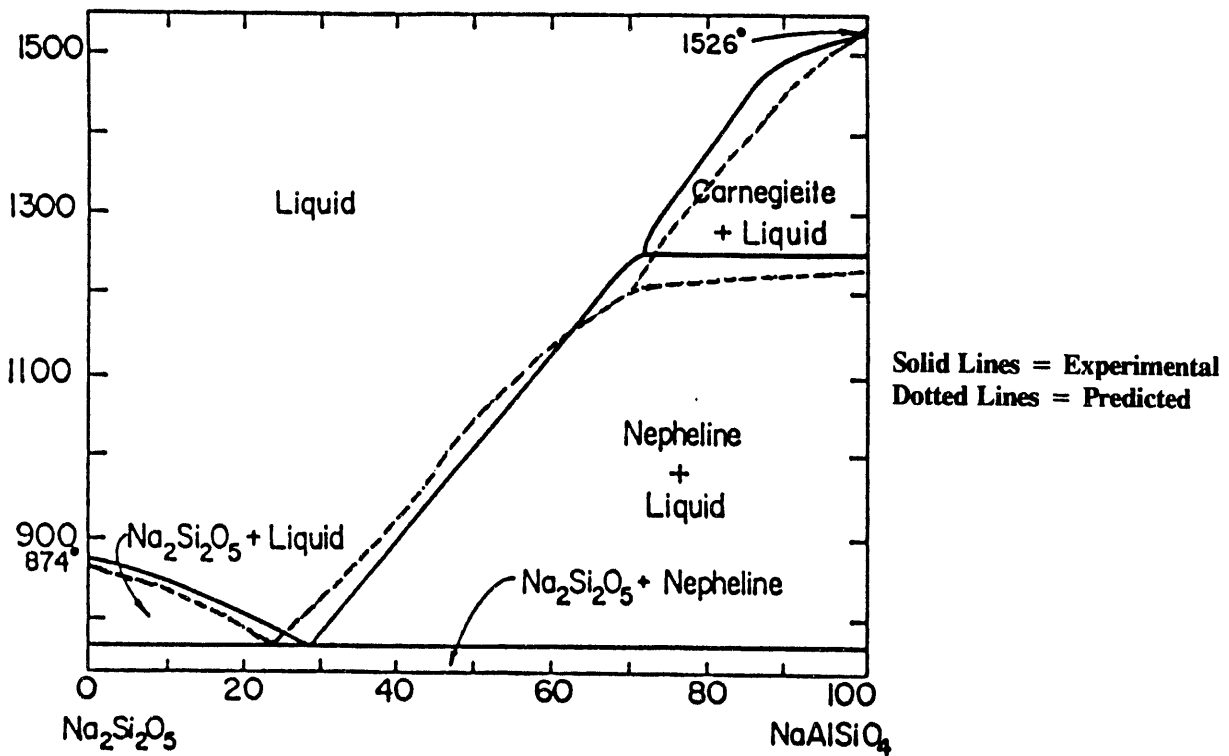


Figure 26. A plot of the experimental vs. predicted phase diagram for Na_2SiO_4 .

work remains unfinished. As soon as the necessary TRTU parameters are identified, the design work on the test loop will be completed. The test loop is expected to be in place and operational in time to be used in conjunction with the initial testing of the TRTU.

High-temperature flange connections for the filter modules are also being designed in order to operate at the extreme conditions of the test loop and to comply with B31.3 piping codes. This will consist of finite element modeling of flange connections to determine thermal stresses and creep phenomena.

5.2 Alkali Gettering

The short-term objective is to construct a coal-water slurry feed system for the PDTF to permit long-duration tests of alkali corrosion of ceramic materials in atmospheric and pressurized coal combustion systems.

5.3 Thermochemical Modeling

No specific task or action item is proposed. Instead, it is expected that PHOEBE will be extensively used as a general tool for the thermodynamic analyses of advanced combustion systems and, specifically, as an optimizer for the selection of alkali gettering materials.

6.0 REFERENCES

1. Lee, S.H.D; Johnson, I. "Removal of Gaseous Alkali Metal Compounds from Hot Flue Gas by Particulate Sorbents," *Journal of Engineering for Power* 1980, 102, 397-402.
2. Punjak, W.A.; Shadman, F. "Aluminosilicate Sorbents for Control of Alkali Vapors During Coal Combustion and Gasification," *Energy and Fuels* 1988, 2 (5), 702-708.
3. Chase, M.W., Jr.; Davies, C.A.; Downey, J.R., Jr.; Frurip, D.J.; McDonald, R.A.; Syverud, A.N. *JANAF Thermochemical Tables*, 3rd ed.; American Chemical Society, NY, 1985.
4. Robie, R.A.; Hemingway, B.S.; Fisher, J.R. "Thermodynamic Properties of Minerals and Related Substances at 285.15 K and 1 Bar (10^5 Pascals) Pressure and at Higher Temperatures," 1978, *U.S. Geol. Surv. Bull.* 1452.
5. Barin, I.; Knacke, O. *Thermochemical Properties of Inorganic Substances*; Springer-Verlag, NY, 1973.
6. Hastie, J.W.; Ondik, H.M.; Bonnell, D.W. "Development of a Ceramic Phase Diagram and Thermodynamic Data Bank," International Conference on the User Applications of Alloy Phase Diagrams, Oct. 4-9, 1988, Lake Buena Vista, FL.
7. Kubaschewski, O.; Alcock, C.B. *Metallurgical Thermochemistry*, 5th ed.; Pergamon Press, NY, 1979.
8. Mayer, J.E.; Mayer, M.G. *Statistical Mechanics*; Wiley, NY, 1957.

9. McBride, B.J.; Gordon, S. "FORTRAN IV Program for Calculation of Thermodynamic Data," NASA TN D-4097, 1967.
10. Ramanathan, M.; Kalmanovitch, D.P.; Ness, S.R. "New Techniques for Thermochemical Equilibria Predictions in Coal Ash Systems - I," *High Temp. Science, An Int'l. Journal* 1989, 28.
11. Ramanathan, M.; Kalmanovitch, D.P. "New Techniques for Thermochemical Equilibria Predictions in Coal Ash Systems II," Conference on High-Temperature Materials Chemistry, ACS Div. Fuel Chemistry, Dallas, TX, 1989.
12. Murnaghan, F.D. *Proc. Natl. Acad. Sci. USA* 1944, 30, 244.

APPENDIX A

FEF DATABASE
**Chemical
Name Index**

No.	Name	Formula
0	2-BUTYNE DINITRILE	C_4N_2 (g)
1	ACETYLENE	C_2H_2 (g)
2	AKERMANITE	$Ca_2MgSi_2O_7$ (s)
3	ALBITE	$NaAlSi_3O_8$ (s,l)
4	ALUMINUM	Al (s,l,g)
5	ALUMINUM CARBIDE	AlC (g)
6	ALUMINUM DICHLORIDE	$AlCl_2$ (g)
7	ALUMINUM DIOXIDE	AlO_2 (g)
8	ALUMINUM HEXACHLORIDE	Al_2Cl_6 (g)
9	ALUMINUM HYDRIDE	AlH (g)
10	ALUMINUM HYDROXIDE	$AlOH$ (g)
11	ALUMINUM MONOCHLORIDE	$AlCl$ (g)
12	ALUMINUM MONOXIDE	AlO (g)
13	ALUMINUM NITRIDE	AlN (s,g)
14	ALUMINUM OXYCHLORIDE	$AlOCl$ (s,g)
15	ALUMINUM SULFATE	$Al_2S_3O_{12}$ (s)
16	ALUMINUM SULFIDE	AlS (g)
17	ALUMINUM SULFIDE	Al_2S_3 (s)
18	ALUMINUM TRICARBIDE	Al_4C_3 (s)
19	ALUMINUM TRICHLORIDE	$AlCl_3$ (s,l,g)
20	AMIDOGEN	NH_2 (g)
21	AMMONIA	NH_3 (g)
22	AMMONIUM CHLORIDE	NH_4Cl (s)
23	AMMONIUM NITRATE	$N_2H_4O_3$ (s)
24	AMMONIUM PERCHLORATE	NH_4ClO_4 (s)
25	ANDALUSITE	Al_2SiO_5 (s)
26	ANHYDRITE	$CaSO_4$ (s)
27	ANORTHITE	$CaAl_2Si_2O_8$ (s,l)
28	ARGON	Ar (g)
29	AZIDE	N_3 (g)
30	BARITE	$BaSO_4$ (s)
31	BARIUM	Ba (s,l,g)
32	BARIUM CHLORIDE	$BaCl$ (g)
33	BARIUM DICHLORIDE	$BaCl_2$ (s,l,g)
34	BARIUM DIHYDROXIDE	BaO_2H_2 (s,l,g)
35	BARIUM MONOHYDROXIDE	$BaOH$ (g)
36	BARIUM OXIDE	BaO (s,l,g)
37	BARIUM SULFIDE	BaS (s,g)
38	BERLINITE	$AlPO_4$ (s)
39	BOEHMITE	AlO_2H (g)
40	CA-AL PYROXENE	$CaAl_2SiO_6$ (s)
41	CALCITE	$CaCO_3$ (s)
42	CALCIUM	Ca (s,l,g)
43	CALCIUM FERRITE	$CaFe_2O_4$ (s)
44	CALCIUM MONOCHLORIDE	$CaCl$ (g)

FEF DATABASE
**Chemical
Name Index**

No.	Name	Formula
45	CALCIUM MONOHYDROXIDE	CaOH (g)
46	CALCIUM NITRATE	CaN ₂ O ₆ (s)
47	CALCIUM OXIDE	CaO (s,l,g)
48	CARBON	C ₂ (g)
49	CARBON	C ₃ (g)
50	CARBON	C ₄ (g)
51	CARBON	C ₅ (g)
52	CARBON	C (s,g)
53	CARBON DIOXIDE	CO ₂ (g)
54	CARBON DISULFIDE	CS ₂ (g)
55	CARBON MONOXIDE	CO (g)
56	CARBON OXIDE SULFIDE	COS (g)
57	CARBON PHOSPHIDE	CP (g)
58	CARBON SUBOXIDE	C ₃ O ₂ (g)
59	CARBON SULFIDE	CS (g)
60	CARBON TETRACHLORIDE	CCl ₄ (g)
61	CARBONIC DICHLORIDE	COCl ₂ (g)
62	CARBONYL CHLORIDE	COCl (g)
63	CHALCOCITE	Cu ₂ S (s)
64	CHLORINE	Cl (g)
65	CHLORINE	Cl ₂ (g)
66	CHLORINE DIOXIDE	ClO ₂ (g)
67	CHLORINE MONOXIDE	ClO (g)
68	CHLOROETHYNE	C ₂ HCl (g)
69	CHLOROMETHANE	CH ₃ Cl (g)
70	CHLOROMETHYLENE	CHCl (g)
71	CHLOROMETHYLIDYNE	CCl (g)
72	CHLOROSILANE	SiH ₃ Cl (g)
73	COHENITE	Fe ₃ C (s)
74	COPPER	Cu (s,l,g)
75	COPPER	Cu ₂ (g)
76	COPPER CYANIDE	CuCN (s)
77	COPPER DICHLORIDE	CuCl ₂ (s)
78	COPPER HYDROXIDE	CuH ₂ O ₂ (s)
79	COPPER MONOCHLORIDE	CuCl (s,l,g)
80	COPPER OXIDE	CuO (s,g)
81	COPPER SULFATE	CuSO ₄ (s)
82	CORDIERITE	Mg ₂ Al ₄ Si ₅ O ₁₈ (s)
83	CORUNDUM	Al ₂ O ₃ (s,l)
84	CUPROUS OXIDE	Cu ₂ O (s,l)
85	CYANOGEN	CN (g)
86	CYANOGEN CHLORIDE	CNCl (g)
87	DIALUMINUM DIOXIDE	Al ₂ O ₂ (g)
88	DIALUMINUM MONOXIDE	Al ₂ O (g)
89	DIAZENE (CIS)	N ₂ H ₂ (g)

FEF DATABASE

Chemical
Name Index

No.	Name	Formula
90	DICALCIUM FERRITE	$\text{Ca}_2\text{Fe}_2\text{O}_5$ (s)
91	DICHLORINE MONOXIDE	Cl_2O (g)
92	DICHLOROETHYNE	C_2Cl_2 (g)
93	DICHLOROMETHANE	CH_2Cl_2 (g)
94	DICHLOROMETHYLENE	CCl_2 (g)
95	DICHLOROSILANE	SiH_2Cl_2 (g)
96	DICOPPER SULFATE	Cu_2SO_5 (s)
97	DIHYDROGEN PHOSPHIDE	H_2P (g)
98	DIIRON HEXACHLORIDE	Fe_2Cl_6 (g)
99	DIIRON TETRACHLORIDE	Fe_2Cl_4 (g)
100	DILITHIUM DICHLORIDE	Li_2Cl_2 (g)
101	DILITHIUM DIHYDROXIDE	$\text{Li}_2\text{H}_2\text{O}_2$ (g)
102	DIMAGNESIUM TETRACHLORIDE	Mg_2Cl_4 (g)
103	DINITROGEN OXIDE	N_2O (g)
104	DINITROGEN PENTAOXIDE	N_2O_5 (g)
105	DINITROGEN TETRAOXIDE	N_2O_4 (s,l,g)
106	DINITROGEN TRIOXIDE	N_2O_3 (g)
107	DIOPSIDE	$\text{CaMgSi}_2\text{O}_6$ (s,l)
108	DIPOTASSIUM CYANIDE	$\text{K}_2\text{C}_2\text{N}_2$ (g)
109	DIPOTASSIUM DICHLORIDE	K_2Cl_2 (g)
110	DIPOTASSIUM DIHYDROXIDE	$\text{K}_2\text{H}_2\text{O}_2$ (g)
111	DISILICON NITRIDE	Si_2N (g)
112	DISODIUM CYANIDE	$\text{Na}_2\text{C}_2\text{N}_2$ (g)
113	DISODIUM DICHLORIDE	Na_2Cl_2 (g)
114	DISODIUM DIHYDROXIDE	$\text{Na}_2\text{H}_2\text{O}_2$ (g)
115	DISULFUR DICHLORIDE	S_2Cl_2 (l,g)
116	DISULFUR MONOCHLORIDE	S_2Cl (g)
117	DISULFUR MONOXIDE	S_2O (g)
118	DOLOMITE	CaMgC_2O_6 (s)
119	ETHANEDINITRILE	C_2N_2 (g)
120	ETHYLENE	C_2H_4 (g)
121	ETHYNYL	C_2H (g)
122	FAYALITE	Fe_2SiO_4 (s)
123	FERRIC SULFATE	$\text{Fe}_2\text{S}_3\text{O}_{12}$ (s)
124	FORMALDEHYDE	CH_2O (g)
125	FORMYL	HCO (g)
126	FORSTERITE	Mg_2SiO_4 (s,l)
127	GEHLENITE	$\text{Ca}_2\text{Al}_2\text{SiO}_7$ (s,l)
128	GROSSULAR	$\text{Ca}_3\text{Al}_2\text{Si}_3\text{O}_{12}$ (s)
129	HEMATITE	Fe_2O_3 (s)
130	HEXACHLOROETHANE	C_2Cl_6 (g)
131	HIGH SANIDINE	KAlSi_3O_8 (s,l)
132	HYDRAZINE	N_2H_4 (l,g)
133	HYDROGEN	H (g)
134	HYDROGEN	H_2 (g)

FEF DATABASE

Chemical
Name Index

No.	Name	Formula
135	HYDROGEN CHLORIDE	HCl (g)
136	HYDROGEN CYANIDE	HCN (g)
137	HYDROGEN ISOCYANATE	HCNO (g)
138	HYDROGEN PEROXIDE	H ₂ O ₂ (g)
139	HYDROGEN PHOSPHIDE	HP (g)
140	HYDROGEN SULFIDE	H ₂ S (g)
141	HYDROPEROXO	HO ₂ (g)
142	HYDROPHILITE	CaCl ₂ (s,l,g)
143	HYDROXYAPATITE	Ca ₅ F ₃ HO ₁₃ (s)
144	HYPOCHLOROUS ACID	HOCl (g)
145	ILMENITE	FeTiO ₃ (s)
146	IMIDOGEN	NH (g)
147	IRON	Fe (s,l,g)
148	IRON CARBONYL	FeC ₅ O ₅ (l,g)
149	IRON DICHLORIDE	FeCl ₂ (s,l,g)
150	IRON HYDROXIDE	FeH ₂ O ₂ (s,g)
151	IRON MONOCHLORIDE	FeCl (g)
152	IRON OXIDE	FeO (s,l,g)
153	IRON SULFATE	FeSO ₄ (s)
154	IRON TRICHLORIDE	FeCl ₃ (s,l,g)
155	IRON TRIHYDROXIDE	FeH ₃ O ₃ (s)
156	JADEITE	NaAlSi ₂ O ₆ (s,l)
157	KALIOPHILLITE	KAlSiO ₄ (s)
158	LARNITE (CA-OLIVINE)	Ca ₂ SiO ₄ (s)
159	LEUCITE	KAlSi ₂ O ₆ (s)
160	LITHIUM	Li (s,l,g)
161	LITHIUM	Li ₂ (g)
162	LITHIUM ALUMINATE	LiAlO ₂ (s,l)
163	LITHIUM CARBIDE	Li ₂ C ₂ (s)
164	LITHIUM CARBONATE	Li ₂ CO ₃ (s,l)
165	LITHIUM DISILICATE	Li ₂ Si ₂ O ₅ (s,l)
166	LITHIUM HYDRIDE	LiH (s,l,g)
167	LITHIUM HYDROXIDE	LiOH (s,l,g)
168	LITHIUM HYPOCHLORITE	LiOCl (g)
169	LITHIUM MONOCHLORIDE	LiCl (s,l,g)
170	LITHIUM MONOXIDE	LiO (g)
171	LITHIUM NITRIDE	LiN (g)
172	LITHIUM OXIDE	Li ₂ O (s,l,g)
173	LITHIUM OXYNITRIDE	LiON (g)
174	LITHIUM PERCHLORATE	LiClO ₄ (s,l)
175	LITHIUM PEROXIDE	Li ₂ O ₂ (s,g)
176	LITHIUM SILICATE	Li ₂ SiO ₃ (s,l)
177	LITHIUM SODIUM OXIDE	LiNaO (g)
178	LITHIUM SULFATE	Li ₂ SO ₄ (s,l,g)
179	LITHIUM TETRAHYDROALUMINATE	LiAlH ₄ (s)

No.	Name	Formula
180	LITHIUM TITANATE	Li_2TiO_3 (s,l)
181	MAGNESIOFERRITE	MgFe_2O_4 (s)
182	MAGNESITE	MgCO_3 (s)
183	MAGNESIUM	Mg (s,l,g)
184	MAGNESIUM	Mg_2 (g)
185	MAGNESIUM CARBIDE	Mg_2C_3 (s)
186	MAGNESIUM CARBIDE	MgC_2 (s)
187	MAGNESIUM DICHLORIDE	MgCl_2 (s,l,g)
188	MAGNESIUM DIHYDRIDE	MgH_2 (s)
189	MAGNESIUM DIHYDROXIDE	MgH_2O_2 (s,g)
190	MAGNESIUM DINITRIDE	Mg_3N_2 (s)
191	MAGNESIUM DITITANATE	MgTi_2O_9 (s,l)
192	MAGNESIUM HYDRIDE	MgH (g)
193	MAGNESIUM HYDROXIDE	MgOH (g)
194	MAGNESIUM MONOCHLORIDE	MgCl (g)
195	MAGNESIUM NITRATE	MgN_2O_6 (s)
196	MAGNESIUM NITRIDE	MgN (g)
197	MAGNESIUM ORTHOTITANATE	Mg_2TiO_4 (s,l)
198	MAGNESIUM OXIDE	MgO (s,l,g)
199	MAGNESIUM PHOSPHATE	$\text{Mg}_3\text{F}_2\text{O}_6$ (s,l)
200	MAGNESIUM SILICATE	MgSiO_3 (s,l)
201	MAGNESIUM SILICIDE	Mg_2Si (s,l)
202	MAGNESIUM SULFATE	MgSO_4 (s,l)
203	MAGNESIUM SULFIDE	MgS (s,g)
204	MAGNESIUM TITANATE	MgTiO_3 (s,l)
205	MAGNETITE	Fe_3O_4 (s)
206	MASCAGNITE	$\text{N}_2\text{H}_6\text{SO}_4$ (s)
207	MERCAPTO	HS (g)
208	MERWINITE	$\text{Ca}_3\text{MgSi}_2\text{O}_6$ (s)
209	METHANE	CH_4 (g)
210	METHINOPHOSPHIDE	CHP (g)
211	METHYL	CH_3 (g)
212	METHYLENE	CH_2 (g)
213	METHYLIDYNE	CH (g)
214	MULLITE	$\text{Al}_6\text{Si}_2\text{O}_{13}$ (s,l)
215	MUSCOVITE	$\text{KAl}_3\text{Si}_3\text{H}_2\text{O}_{12}$ (s)
216	NEPHELINE	NaAlSiO_4 (s,l)
217	NITER	KNO_3 (s)
218	NITRIC ACID	HNO_3 (g)
219	NITROBARITE	BaN_2O_6 (s)
220	NITROGEN	N (g)
221	NITROGEN	N_2 (g)
222	NITROGEN DIOXIDE	NO_2 (g)
223	NITROGEN MONOXIDE	NO (g)
224	NITROGEN TRIOXIDE	NO_3 (g)

No.	Name	Formula
225	NITROSYL CHLORIDE	NOCl (g)
226	NITROUS ACID	$\text{HNO}_2 \text{ (g)}$
227	NITROXYL	HNO (g)
228	NITRYL CHLORIDE	$\text{NO}_2\text{Cl (g)}$
229	OLDHAMITE	CaS (s,g)
230	OXIRANE	$\text{C}_2\text{H}_4\text{O (g)}$
231	OXYGEN	O (g)
232	OXYGEN	$\text{O}_2 \text{ (g)}$
233	OZONE	$\text{O}_3 \text{ (g)}$
234	PEROVSKITE	$\text{CaTiO}_3 \text{ (s)}$
235	PHOSPHORIC ACID	$\text{H}_3\text{PO}_4 \text{ (s,l)}$
236	PHOSPHOROUS MONOCHLORIDE	PCl (g)
237	PHOSPHORUS	P (s,l,g)
238	PHOSPHORUS	$\text{P}_2 \text{ (g)}$
239	PHOSPHORUS	$\text{P}_4 \text{ (g)}$
240	PHOSPHORUS DIOXIDE	$\text{PO}_2 \text{ (g)}$
241	PHOSPHORUS MONOXIDE	PO (g)
242	PHOSPHORUS NITRIDE	PN (g)
243	PHOSPHORUS PENTACHLORIDE	$\text{PCl}_5 \text{ (g)}$
244	PHOSPHORUS PENTAOXIDE DIMER	$\text{P}_4\text{O}_{10} \text{ (s,g)}$
245	PHOSPHORUS SULFIDE	PS (g)
246	PHOSPHORUS TRICHLORIDE	$\text{PCl}_3 \text{ (g)}$
247	PHOSPHORUS TRIOXIDE DIMER	$\text{P}_4\text{O}_6 \text{ (g)}$
248	PHOSPHORUS TRISULFIDE	$\text{P}_4\text{S}_3 \text{ (s,l,g)}$
249	PHOSPHORYL TRICHLORIDE	$\text{POCl}_3 \text{ (g)}$
250	PORTLANDITE	$\text{CaO}_2\text{H}_2 \text{ (s,g)}$
251	POTASSIUM	K (s,l,g)
252	POTASSIUM	$\text{K}_2 \text{ (g)}$
253	POTASSIUM ALUMINUM SULFATE	$\text{KAlS}_2\text{O}_6 \text{ (s)}$
254	POTASSIUM CARBONATE	$\text{K}_2\text{CO}_3 \text{ (s,l)}$
255	POTASSIUM CHLORIDE	KCl (s,l,g)
256	POTASSIUM CYANIDE	KCN (s,l,g)
257	POTASSIUM DIOXIDE	$\text{KO}_2 \text{ (s)}$
258	POTASSIUM HEXACHLOROALUMINATE	$\text{K}_3\text{AlCl}_6 \text{ (s)}$
259	POTASSIUM HYDRIDE	KH (s,g)
260	POTASSIUM HYDROXIDE	KOH (s,l,g)
261	POTASSIUM MONOXIDE	KO (g)
262	POTASSIUM NANOCHLOROALUMINATE	$\text{K}_3\text{Al}_2\text{Cl}_7 \text{ (s)}$
263	POTASSIUM OXIDE	$\text{K}_2\text{O (s)}$
264	POTASSIUM PERCHLORATE	$\text{KClO}_4 \text{ (s)}$
265	POTASSIUM PEROXIDE	$\text{K}_2\text{O}_2 \text{ (s)}$
266	POTASSIUM SILICATE	$\text{K}_2\text{SiO}_3 \text{ (s,l)}$
267	POTASSIUM SULFATE	$\text{K}_2\text{SO}_4 \text{ (s,l,g)}$
268	POTASSIUM SULFIDE	$\text{K}_2\text{S (s,l)}$
269	POTASSIUM TETRACHLOROALUMINATE	$\text{KAlCl}_4 \text{ (s)}$

FEF DATABASE

Chemical
Name Index

No.	Name	Formula
270	PYRITE	FeS ₂ (s)
271	PYROPE	Mg ₃ Al ₂ Si ₃ O ₁₂ (s)
272	PYROPHYLLITE	Al ₂ Si ₄ H ₂ O ₁₂ (s)
273	FYRRHOTITE	Fe _{0.877} S (s)
274	RUTILE	TiO ₂ (s,l,g)
275	SILICON	Si (s,l,g)
276	SILICON	Si ₂ (g)
277	SILICON	Si ₃ (g)
278	SILICON CARBIDE	SiC (s,g)
279	SILICON DICARBIDE	SiC ₂ (g)
280	SILICON DICHLORIDE	SiCl ₂ (g)
281	SILICON DIOXIDE	SiO ₂ (s,l,g)
282	SILICON DISULFIDE	SiS ₂ (s,l)
283	SILICON HYDRIDE	SiH (g)
284	SILICON MONOCHLORIDE	SiCl (g)
285	SILICON MONOXIDE	SiO (g)
286	SILICON NITRIDE	SiN (g)
287	SILICON SULFIDE	SiS (g)
288	SILICON TETRACHLORIDE	SiCl ₄ (g)
289	SILICON TETRAHYDRIDE	SiH ₄ (g)
290	SILICON TRICHLORIDE	SiCl ₃ (g)
291	SODIUM	Na (s,l,g)
292	SODIUM	Na ₂ (g)
293	SODIUM ALUMINATE	NaAlO ₂ (s)
294	SODIUM CARBONATE	Na ₂ CO ₃ (s,l)
295	SODIUM CHLORIDE	NaCl (s,l,g)
296	SODIUM CYANIDE	NaCN (s,l,g)
297	SODIUM DIOXIDE	NaO ₂ (s)
298	SODIUM DISILICATE	Na ₂ Si ₂ O ₅ (s,l)
299	SODIUM DISULFIDE	Na ₂ S ₂ (s,l)
300	SODIUM HEXACHLOROALUMINATE	Na ₃ AlCl ₆ (s)
301	SODIUM HYDRIDE	NaH (s,g)
302	SODIUM HYDROXIDE	NaOH (s,l,g)
303	SODIUM MONOXIDE	NaO (g)
304	SODIUM OXIDE	Na ₂ O (s,l)
305	SODIUM PERCHLORATE	NaClO ₄ (s)
306	SODIUM PEROXIDE	Na ₂ O ₂ (s)
307	SODIUM SILICATE	Na ₂ SiO ₃ (s,l)
308	SODIUM SULFATE	Na ₂ SO ₄ (s,l,g)
309	SODIUM SULFIDE	Na ₂ S (s,l)
310	SODIUM TETRACHLOROALUMINATE	NaAlCl ₄ (s)
311	SPINEL	MgAl ₂ O ₄ (s,l)
312	SULFUR	S (s,l,g)
313	SULFUR	S ₂ (g)
314	SULFUR	S ₃ (g)

No.	Name	Formula
315	SULFUR	S ₄ (g)
316	SULFUR	S ₅ (g)
317	SULFUR	S ₆ (g)
318	SULFUR	S ₇ (g)
319	SULFUR	S ₈ (g)
320	SULFUR DICHLORIDE	SCl ₂ (l,g)
321	SULFUR DIOXIDE	SO ₂ (g)
322	SULFUR MONOCHLORIDE	SCl (g)
323	SULFUR MONOXIDE	SO (g)
324	SULFUR NITRIDE	SN (g)
325	SULFUR TRIOXIDE	SO ₃ (g)
326	SULFURIC ACID	H ₂ SO ₄ (l,g)
327	SULFURIC ACID DIHYDRATE	H ₂ SO ₄ (l)
328	SULFURIC ACID HEMIHEXAHYDRATE	H _{1.5} SO _{10.500} (l)
329	SULFURIC ACID MONOHYDRATE	H ₄ SO ₅ (l)
330	SULFURIC ACID TETRAHYDRATE	H ₁₀ SO ₆ (l)
331	SULFURIC ACID TRIHYDRATE	H ₆ SO ₇ (l)
332	SULFURYL CHLORIDE	SO ₂ Cl ₂ (g)
333	TETRACHLOROETHYLENE	C ₂ Cl ₄ (g)
334	TETRAMETHYLSILANE	SiC ₄ H ₁₂ (g)
335	THIOPHOSPHORYL TRICHLORIDE	SPhCl ₃ (g)
336	TITANITE (SPHENE)	CaTiSiO ₅ (s)
337	TITANIUM	Ti (s,l,g)
338	TITANIUM CARBIDE	TiC (s,l)
339	TITANIUM DICHLORIDE	TiCl ₂ (s,g)
340	TITANIUM HYDRIDE	TiH ₂ (s)
341	TITANIUM HYPOCHLORATE	TiOCl ₂ (g)
342	TITANIUM HYPOCHLORITE	TiOCl (g)
343	TITANIUM MONOCHLORIDE	TiCl (s)
344	TITANIUM MONOXIDE	TiO (s,l,g)
345	TITANIUM NITRIDE	TiN (s,l)
346	TITANIUM OXIDE	Ti ₂ O ₃ (s,l)
347	TITANIUM PENTAOXIDE	Ti ₃ O ₅ (s,l)
348	TITANIUM SEPTOXIDE	Ti ₄ O ₇ (s,l)
349	TITANIUM TETRACHLORIDE	TiCl ₄ (s,l,g)
350	TITANIUM TRICHLORIDE	TiCl ₃ (s,g)
351	TREMOLITE	Ca ₂ Mg ₅ Si ₈ H ₂ O ₂₄ (s)
352	TRICHLOROMETHANE	CHCl ₃ (g)
353	TRICHLOROMETHYL	CCl ₃ (g)
354	TRICHLOROMETHYLSILANE	SiCH ₃ Cl ₃ (g)
355	TRICHLOROSILANE	SiHCl ₃ (g)
356	TRICOPPER TRICHLORIDE	Cu ₃ Cl ₃ (g)
357	TRIHYDROGEN PHOSPHIDE	H ₃ P (g)
358	TRILITHIUM NITRIDE	Li ₃ N (s)
359	TRILITHIUM TRICHLORIDE	Li ₃ Cl ₃ (g)

FEF DATABASE

*Chemical
Name Index*

No.	Name	Formula
360	TRIPHOSPHORUS PENTANITRIDE	P_3N_5 (s)
361	TRISILICON TETRANITRIDE	Si_3N_4 (s)
362	TROILITE	FeS (s,l,g)
363	WATER	H ₂ O (l,g)
364	WHITLOCKITE	Ca ₃ F ₂ O ₈ (s)
365	WITHERITE	BaCO ₃ (s)
366	WOLLASTONITE	CaSiO ₃ (s)
367	WUSTITE	Fe _{0.947} O (s)

APPENDIX B

No.	Formula	Name
0	Al	ALUMINUM (s,l,g)
1	AlC	ALUMINUM CARBIDE (g)
2	AlCl	ALUMINUM MONOCHLORIDE (g)
3	AlCl ₂	ALUMINUM DICHLORIDE (g)
4	AlCl ₃	ALUMINUM TRICHLORIDE (s,l,g)
5	AlH	ALUMINUM HYDRIDE (g)
6	AlN	ALUMINUM NITRIDE (s,g)
7	AlO	ALUMINUM MONOXIDE (g)
8	AlOCl	ALUMINUM OXYCHLORIDE (s,g)
9	AlOH	ALUMINUM HYDROXIDE (g)
10	AlO ₂	ALUMINUM DIOXIDE (g)
11	AlO ₂ H	BOEHMITE (g)
12	AlPO ₄	BERLINITE (s)
13	AlS	ALUMINUM SULFIDE (g)
14	Al ₂ Cl ₆	ALUMINUM HEXACHLORIDE (g)
15	Al ₂ O	DIALUMINUM MONOXIDE (g)
16	Al ₂ O ₂	DIALUMINUM DIOXIDE (g)
17	Al ₂ O ₃	CORUNDUM (s,l)
18	Al ₂ S ₃	ALUMINUM SULFIDE (s)
19	Al ₂ S ₃ O ₁₂	ALUMINUM SULFATE (s)
20	Al ₂ SiO ₅	ANDALUSITE (s)
21	Al ₂ Si ₄ H ₂ O ₁₂	PYROPHYLLITE (s)
22	Al ₄ C ₃	ALUMINUM TRICARBIDE (s)
23	Al ₆ Si ₂ O ₁₃	MULLITE (s,l)
24	Ar	ARGON (g)
25	Ba	BARIUM (s,l,g)
26	BaCO ₃	WITHERITE (s)
27	BaCl	BARIUM CHLORIDE (g)
28	BaCl ₂	BARIUM DICHLORIDE (s,l,g)
29	BaN ₂ O ₆	NITROBARITE (s)
30	BaO	BARIUM OXIDE (s,l,g)
31	BaOH	BARIUM MONOHYDROXIDE (g)
32	BaO ₂ H ₂	BARIUM DIHYDROXIDE (s,l,g)
33	BaS	BARIUM SULFIDE (s,g)
34	BaSO ₄	BARITE (s)
35	C	CARBON (s,g)
36	CCl	CHLOROMETHYLIDYNE (g)
37	CCl ₂	DICHLOROMETHYLENE (g)
38	CCl ₃	TRICHLOROMETHYL (g)
39	CCl ₄	CARBON TETRACHLORIDE (g)
40	CH	METHYLIDYNE (g)
41	CHCl	CHLOROMETHYLENE (g)
42	CHCl ₃	TRICHLOROMETHANE (g)
43	CHP	METHINOPHOSPHIDE (g)
44	CH ₂	METHYLENE (g)

No.	Formula	Name
45	CH ₂ Cl ₂	DICHLOROMETHANE (g)
46	CH ₂ O	FORMALDEHYDE (g)
47	CH ₃	METHYL (g)
48	CH ₃ Cl	CHLOROMETHANE (g)
49	CH ₄	METHANE (g)
50	CN	CYANOGEN (g)
51	CNCl	CYANOGEN CHLORIDE (g)
52	CO	CARBON MONOXIDE (g)
53	COCl	CARBONYL CHLORIDE (g)
54	COCl ₂	CARBONIC DICHLORIDE (g)
55	COS	CARBON OXIDE SULFIDE (g)
56	CO ₂	CARBON DIOXIDE (g)
57	CP	CARBON PHOSPHIDE (g)
58	CS	CARBON SULFIDE (g)
59	CS ₂	CARBON DISULFIDE (g)
60	C ₂	CARBON (g)
61	C ₂ Cl ₂	DICHLOROETHYNE (g)
62	C ₂ Cl ₄	TETRACHLOROETHYLENE (g)
63	C ₂ Cl ₆	HEXACHLOROETHANE (g)
64	C ₂ H	ETHYNYL (g)
65	C ₂ HCl	CHLOROETHYNE (g)
66	C ₂ H ₂	ACETYLENE (g)
67	C ₂ H ₄	ETHYLENE (g)
68	C ₂ H ₄ O	OXIRANE (g)
69	C ₂ N ₂	ETHANEDINITRILE (g)
70	C ₃	CARBON (g)
71	C ₃ O ₂	CARBON SUBOXIDE (g)
72	C ₄	CARBON (g)
73	C ₄ N ₂	2-BUTYNE DINITRILE (g)
74	C ₅	CARBON (g)
75	Ca	CALCIUM (s,l,g)
76	CaAl ₂ SiO ₆	CA-AL PYROXENE (s)
77	CaAl ₂ Si ₂ O ₈	ANORTHITE (s,l)
78	CaCO ₃	CALCITE (s)
79	CaCl	CALCIUM MONOCHLORIDE (g)
80	CaCl ₂	HYDROPHILITE (s,l,g)
81	CaFe ₂ O ₄	CALCIUM FERRITE (s)
82	CaMgC ₂ O ₆	DOLOMITÉ (s)
83	CaMgSi ₂ O ₆	DIOPSIDE (s,l)
84	CaN ₂ O ₆	CALCIUM NITRATE (s)
85	CaO	CALCIUM OXIDE (s,l,g)
86	CaOH	CALCIUM MONOHYDROXIDE (g)
87	CaO ₂ H ₂	PORTLANDITE (s,g)
88	CaS	OLDHAMITE (s,g)
89	CaSO ₄	ANHYDRITE (s)

No.	Formula	Name
90	CaSiO ₃	WOLLASTONITE (s)
91	CaTiO ₃	PEROVSKITE (s)
92	CaTiSiO ₅	TITANITE (SPHENE) (s)
93	Ca ₂ Al ₂ SiO ₇	GEHLENITE (s,l)
94	Ca ₂ Fe ₂ O ₅	DICALCIUM FERRITE (s)
95	Ca ₂ MgSi ₂ O ₇	AKERMANITE (s)
96	Ca ₂ Mg ₅ Si ₈ H ₂ O ₂₄	TREMOLITE (s)
97	Ca ₂ SiO ₄	LARNITE (CA-OLIVINE) (s)
98	Ca ₃ Al ₂ Si ₃ O ₁₂	GROSSULAR (s)
99	Ca ₃ MgSi ₂ O ₈	MERWINITE (s)
100	Ca ₃ F ₂ O ₈	WHITLOCKITE (s)
101	Ca ₃ F ₃ HO ₁₃	HYDROXYAPATITE (s)
102	Cl	CHLORINE (g)
103	ClO	CHLORINE MONOXIDE (g)
104	ClO ₂	CHLORINE DIOXIDE (g)
105	Cl ₂	CHLORINE (g)
106	Cl ₂ O	DICHLORINE MONOXIDE (g)
107	Cu	COPPER (s,l,g)
108	CuCN	COPPER CYANIDE (s)
109	CuCl	COPPER MONOCHLORIDE (s,l,g)
110	CuCl ₂	COPPER DICHLORIDE (s)
111	CuH ₂ O ₂	COPPER HYDROXIDE (s)
112	CuO	COPPER OXIDE (s,g)
113	CuSO ₄	COPPER SULFATE (s)
114	Cu ₂	COPPER (g)
115	Cu ₂ O	CUPROUS OXIDE (s,l)
116	Cu ₂ S	CHALCOCITE (s)
117	Cu ₂ SO ₅	DICOPPER SULFATE (s)
118	Cu ₃ Cl ₃	TRICOPPER TRICHLORIDE (g)
119	Fe _{0.877} S	PYRRHOTITE (s)
120	Fe _{0.947} O	WUSTITE (s)
121	Fe	IRON (s,l,g)
122	FeC ₅ O ₅	IRON CARBONYL (l,g)
123	FeCl	IRON MONOCHLORIDE (g)
124	FeCl ₂	IRON DICHLORIDE (s,l,g)
125	FeCl ₃	IRON TRICHLORIDE (s,l,g)
126	FeH ₂ O ₂	IRON HYDROXIDE (s,g)
127	FeH ₃ O ₃	IRON TRIHYDROXIDE (s)
128	FeO	IRON OXIDE (s,l,g)
129	FeS	TROILITE (s,l,g)
130	FeSO ₄	IRON SULFATE (s)
131	FeS ₂	PYRITE (s)
132	FeTiO ₃	ILMENITE (s)
133	Fe ₂ Cl ₄	DIIRON TETRACHLORIDE (g)
134	Fe ₂ Cl ₆	DIIRON HEXACHLORIDE (g)

No.	Formula	Name
135	Fe ₂ O ₃	HEMATITE (s)
136	Fe ₂ S ₃ O ₁₂	FERRIC SULFATE (s)
137	Fe ₂ SiO ₄	FAYALITE (s)
138	Fe ₃ C	COHENITE (s)
139	Fe ₃ O ₄	MAGNETITE (s)
140	H	HYDROGEN (g)
141	HCN	HYDROGEN CYANIDE (g)
142	HCNO	HYDROGEN ISOCYANATE (g)
143	HCO	FORMYL (g)
144	HCl	HYDROGEN CHLORIDE (g)
145	HNO	NITROXYL (g)
146	HNO ₂	NITROUS ACID (g)
147	HNO ₃	NITRIC ACID (g)
148	HOCl	HYPOCHLOROUS ACID (g)
149	HO ₂	HYDROPEROXO (g)
150	HP	HYDROGEN PHOSPHIDE (g)
151	HS	MERCAPTO (g)
152	H ₂	HYDROGEN (g)
153	H ₂ O	WATER (l,g)
154	H ₂ O ₂	HYDROGEN PEROXIDE (g)
155	H ₂ P	DIHYDROGEN PHOSPHIDE (g)
156	H ₂ S	HYDROGEN SULFIDE (g)
157	H ₂ SO ₄	SULFURIC ACID (l,g)
158	H ₃ P	TRIHYDROGEN PHOSPHIDE (g)
159	H ₃ PO ₄	PHOSPHORIC ACID (s,l)
160	H ₄ SO ₅	SULFURIC ACID MONOHYDRATE (l)
161	H ₄ SO ₆	SULFURIC ACID DIHYDRATE (l)
162	H ₆ SO ₇	SULFURIC ACID TRIHYDRATE (l)
163	H ₁₀ SO ₈	SULFURIC ACID TETRAHYDRATE (l)
164	H ₁₅ SO _{10.500}	SULFURIC ACID HEMIHEXAHYDRATE (l)
165	K	POTASSIUM (s,l,g)
166	KAlCl ₄	POTASSIUM TETRACHLOROALUMINATE (s)
167	KAlS ₂ O ₆	POTASSIUM ALUMINUM SULFATE (s)
168	KAlSiO ₄	KALIOPHILLITE (s)
169	KAlSi ₂ O ₆	LEUCITE (s)
170	KAlSi ₃ O ₈	HIGH SANIDINE (s,l)
171	KAl ₃ Si ₃ H ₂ O ₁₂	MUSCOVITE (s)
172	KCN	POTASSIUM CYANIDE (s,l,g)
173	KCl	POTASSIUM CHLORIDE (s,l,g)
174	KClO ₄	POTASSIUM PERCHLORATE (s)
175	KH	POTASSIUM HYDRIDE (s,g)
176	KNO ₃	NITER (s)
177	KO	POTASSIUM MONOXIDE (g)
178	KOH	POTASSIUM HYDROXIDE (s,l,g)
179	KO ₂	POTASSIUM DIOXIDE (s)

No.	Formula	Name
180	K_2	POTASSIUM (g)
181	K_2CO_3	POTASSIUM CARBONATE (s,1)
182	$K_2C_2N_2$	DIPOTASSIUM CYANIDE (g)
183	K_2Cl_2	DIPOTASSIUM DICHLORIDE (g)
184	$K_2H_2O_2$	DIPOTASSIUM DIHYDROXIDE (g)
185	K_2O	POTASSIUM OXIDE (s)
186	K_2O_2	POTASSIUM PEROXIDE (s)
187	K_2S	POTASSIUM SULFIDE (s,1)
188	K_2SO_4	POTASSIUM SULFATE (s,1,g)
189	K_2SiO_3	POTASSIUM SILICATE (s,1)
190	K_6AlCl_6	POTASSIUM HEXACHLOROALUMINATE (s)
191	$K_3Al_2Cl_7$	POTASSIUM NANOCHLOROALUMINATE (s)
192	Li	LITHIUM (s,1,g)
193	$LiAlH_4$	LITHIUM TETRAHYDROALUMINATE (s)
194	$LiAlO_2$	LITHIUM ALUMINATE (s,1)
195	LiCl	LITHIUM MONOCHLORIDE (s,1,g)
196	$LiClO_4$	LITHIUM PERCHLORATE (s,1)
197	LiH	LITHIUM HYDRIDE (s,1,g)
198	LiN	LITHIUM NITRIDE (g)
199	LiNaO	LITHIUM SODIUM OXIDE (g)
200	LiO	LITHIUM MONOXIDE (g)
201	LiOCl	LITHIUM HYPOCHLORITE (g)
202	LiOH	LITHIUM HYDROXIDE (s,1,g)
203	LiON	LITHIUM OXYNITRIDE (g)
204	Li ₂	LITHIUM (g)
205	Li_2CO_3	LITHIUM CARBONATE (s,1)
206	Li_2C_2	LITHIUM CARBIDE (s)
207	Li_2Cl_2	DILITHIUM DICHLORIDE (g)
208	$Li_2H_2O_2$	DILITHIUM DIHYDROXIDE (g)
209	Li_2O	LITHIUM OXIDE (s,1,g)
210	Li_2O_2	LITHIUM PEROXIDE (s,g)
211	Li_2SO_4	LITHIUM SULFATE (s,1,g)
212	Li_2SiO_3	LITHIUM SILICATE (s,1)
213	$Li_2Si_2O_5$	LITHIUM DISILICATE (s,1)
214	Li_2TiO_3	LITHIUM TITANATE (s,1)
215	Li_3Cl_3	TRILITHIUM TRICHLORIDE (g)
216	Li_3N	TRILITHIUM NITRIDE (s)
217	Mg	MAGNESIUM (s,1,g)
218	$MgAl_2O_4$	SPINEL (s,1)
219	$MgCO_3$	MAGNESITE (s)
220	MgC_2	MAGNESIUM CARBIDE (s)
221	MgCl	MAGNESIUM MONOCHLORIDE (g)
222	$MgCl_2$	MAGNESIUM DICHLORIDE (s,1,g)
223	$MgFe_2O_4$	MAGNESIOFERRITE (s)
224	MgH	MAGNESIUM HYDRIDE (g)

No.	Formula	Name
225	MgH ₂	MAGNESIUM DIHYDRIDE (s)
226	MgH ₂ O ₂	MAGNESIUM DIHYDROXIDE (s,g)
227	MgN	MAGNESIUM NITRIDE (g)
228	MgN ₂ O ₆	MAGNESIUM NITRATE (s)
229	MgO	MAGNESIUM OXIDE (s,l,g)
230	MgOH	MAGNESIUM HYDROXIDE (g)
231	MgS	MAGNESIUM SULFIDE (s,g)
232	MgSO ₄	MAGNESIUM SULFATE (s,l)
233	MgSiO ₃	MAGNESIUM SILICATE (s,l)
234	MgTiO ₃	MAGNESIUM TITANATE (s,l)
235	MgTi ₂ O ₅	MAGNESIUM DITITANATE (s,l)
236	Mg ₂	MAGNESIUM (g)
237	Mg ₂ Al ₄ Si ₅ O ₁₈	CORDIERITE (s)
238	Mg ₂ C ₃	MAGNESIUM CARBIDE (s)
239	Mg ₂ Cl ₄	DIMAGNESIUM TETRACHLORIDE (g)
240	Mg ₂ Si	MAGNESIUM SILICIDE (s,l)
241	Mg ₂ SiO ₄	FORSTERITE (s,l)
242	Mg ₂ TiO ₄	MAGNESIUM ORTHOTITANATE (s,l)
243	Mg ₃ Al ₂ Si ₃ O ₁₂	PYROPE (s)
244	Mg ₃ N ₂	MAGNESIUM DINITRIDE (s)
245	Mg ₃ P ₂ O ₈	MAGNESIUM PHOSPHATE (s,l)
246	N	NITROGEN (g)
247	NH	IMIDOGEN (g)
248	NH ₂	AMIDOGEN (g)
249	NH ₃	AMMONIA (g)
250	NH ₄ Cl	AMMONIUM CHLORIDE (s)
251	NH ₄ ClO ₄	AMMONIUM PERCHLORATE (s)
252	NO	NITROGEN MONOXIDE (g)
253	NOCl	NITROSYL CHLORIDE (g)
254	NO ₂	NITROGEN DIOXIDE (g)
255	NO ₂ Cl	NITRYL CHLORIDE (g)
256	NO ₃	NITROGEN TRIOXIDE (g)
257	N ₂	NITROGEN (g)
258	N ₂ H ₂	DIAZENE (CIS) (g)
259	N ₂ H ₄	HYDRAZINE (l,g)
260	N ₂ H ₄ O ₃	AMMONIUM NITRATE (s)
261	N ₂ H ₆ SO ₄	MASCAGNITE (s)
262	N ₂ O	DINITROGEN OXIDE (g)
263	N ₂ O ₃	DINITROGEN TRIOXIDE (g)
264	N ₂ O ₄	DINITROGEN TETRAOXIDE (s,l,g)
265	N ₂ O ₅	DINITROGEN PENTAOXIDE (g)
266	N ₃	AZIDE (g)
267	Na	SODIUM (s,l,g)
268	NaAlCl ₄	SODIUM TETRACHLOROALUMINATE (s)
269	NaAlO ₂	SODIUM ALUMINATE (s)

No.	Formula	Name
270	NaAlSiO ₄	NEPHELINE (s,l)
271	NaAlSi ₂ O ₆	JADEITE (s,l)
272	NaAlSi ₃ O ₈	ALBITE (s,l)
273	NaCN	SODIUM CYANIDE (s,l,g)
274	NaCl	SODIUM CHLORIDE (s,l,g)
275	NaClO ₄	SODIUM PERCHLORATE (s)
276	NaH	SODIUM HYDRIDE (s,g)
277	NaO	SODIUM MONOXIDE (g)
278	NaOH	SODIUM HYDROXIDE (s,l,g)
279	NaO ₂	SODIUM DIOXIDE (s)
280	Na ₂	SODIUM (g)
281	Na ₂ CO ₃	SODIUM CARBONATE (s,l)
282	Na ₂ C ₂ N ₂	DISODIUM CYANIDE (g)
283	Na ₂ Cl ₂	DISODIUM DICHLORIDE (g)
284	Na ₂ H ₂ O ₂	DISODIUM DIHYDROXIDE (g)
285	Na ₂ O	SODIUM OXIDE (s,l)
286	Na ₂ O ₂	SODIUM PEROXIDE (s)
287	Na ₂ S	SODIUM SULFIDE (s,l)
288	Na ₂ SO ₄	SODIUM SULFATE (s,l,g)
289	Na ₂ S ₂	SODIUM DISULFIDE (s,l)
290	Na ₂ SiO ₃	SODIUM SILICATE (s,l)
291	Na ₂ Si ₂ O ₅	SODIUM DISILICATE (s,l)
292	Na ₃ AlCl ₄	SODIUM HEXACHLOROALUMINATE (s)
293	O	OXYGEN (g)
294	O ₂	OXYGEN (g)
295	O ₃	OZONE (g)
296	P	PHOSPHORUS (s,l,g)
297	PCl	PHOSPHOROUS MONOCHLORIDE (g)
298	PCl ₃	PHOSPHORUS TRICHLORIDE (g)
299	PCl ₅	PHOSPHORUS PENTACHLORIDE (g)
300	PN	PHOSPHORUS NITRIDE (g)
301	PO	PHOSPHORUS MONOXIDE (g)
302	POCl ₃	PHOSPHORYL TRICHLORIDE (g)
303	PO ₂	PHOSPHORUS DIOXIDE (g)
304	PS	PHOSPHORUS SULFIDE (g)
305	P ₂	PHOSPHORUS (g)
306	P ₃ N ₅	TRIPHOSPHORUS PENTANITRIDE (s)
307	P ₄	PHOSPHORUS (g)
308	P ₄ O ₆	PHOSPHORUS TRIOXIDE DIMER (g)
309	P ₄ O ₁₀	PHOSPHORUS PENTAOXIDE DIMER (s,g)
310	P ₄ S ₃	PHOSPHORUS TRISULFIDE (s,l,g)
311	S	SULFUR (s,l,g)
312	SCl	SULFUR MONOCHLORIDE (g)
313	SCl ₂	SULFUR DICHLORIDE (l,g)
314	SN	SULFUR NITRIDE (g)

No.	Formula	Name
315	SO	SULFUR MONOXIDE (g)
316	SO ₂	SULFUR DIOXIDE (g)
317	SO ₂ Cl ₂	SULFURYL CHLORIDE (g)
318	SO ₃	SULFUR TRIOXIDE (g)
319	SPOCl ₃	THIOPHOSPHORYL TRICHLORIDE (g)
320	S ₂	SULFUR (g)
321	S ₂ Cl	DISULFUR MONOCHLORIDE (g)
322	S ₂ Cl ₂	DISULFUR DICHLORIDE (l,g)
323	S ₂ O	DISULFUR MONOXIDE (g)
324	S ₃	SULFUR (g)
325	S ₄	SULFUR (g)
326	S ₅	SULFUR (g)
327	S ₆	SULFUR (g)
328	S ₇	SULFUR (g)
329	S ₈	SULFUR (g)
330	Si	SILICON (s,l,g)
331	SiC	SILICON CARBIDE (s,g)
332	SiCH ₃ Cl ₃	TRICHLOROMETHYLSILANE (g)
333	SiC ₂	SILICON DICARBIDE (g)
334	SiC ₄ H ₁₂	TETRAMETHYLSILANE (g)
335	SiCl	SILICON MONOCHLORIDE (g)
336	SiCl ₂	SILICON DICHLORIDE (g)
337	SiCl ₃	SILICON TRICHLORIDE (g)
338	SiCl ₄	SILICON TETRACHLORIDE (g)
339	SiH	SILICON HYDRIDE (g)
340	SiHCl ₃	TRICHLOROSILANE (g)
341	SiH ₂ Cl ₂	DICHLOROSILANE (g)
342	SiH ₃ Cl	CHLOROSILANE (g)
343	SiH ₄	SILICON TETRAHYDRIDE (g)
344	SiN	SILICON NITRIDE (g)
345	SiO	SILICON MONOXIDE (g)
346	SiO ₂	SILICON DIOXIDE (s,l,g)
347	SiS	SILICON SULFIDE (g)
348	SiS ₂	SILICON DISULFIDE (s,l)
349	Si ₂	SILICON (g)
350	Si ₂ N	DISILICON NITRIDE (g)
351	Si ₃	SILICON (g)
352	Si ₃ N ₄	TRISILICON TETRANITRIDE (s)
353	Ti	TITANIUM (s,l,g)
354	TiC	TITANIUM CARBIDE (s,l)
355	TiCl	TITANIUM MONOCHLORIDE (s)
356	TiCl ₂	TITANIUM DICHLORIDE (s,g)
357	TiCl ₃	TITANIUM TRICHLORIDE (s,g)
358	TiCl ₄	TITANIUM TETRACHLORIDE (s,l,g)
359	TiH ₂	TITANIUM HYDRIDE (s)

No.	Formula	Name
360	TiN	TITANIUM NITRIDE (s,l)
361	TiO	TITANIUM MONOXIDE (s,l,g)
362	TiOCl	TITANIUM HYPOCHLORITE (g)
363	TiOCl ₂	TITANIUM HYPOCHLORATE (g)
364	TiO ₂	RUTILE (s,l,g)
365	Ti ₂ O ₃	TITANIUM OXIDE (s,l)
366	Ti ₃ O ₅	TITANIUM PENTAOXIDE (s,l)
367	Ti ₄ O ₇	TITANIUM SEPTOXIDE (s,l)

U.S. DEPARTMENT OF ENERGY
FEDERAL ASSISTANCE MANAGEMENT SUMMARY REPORT

1. Program/Project Identification No. DE-FC21-86MC10637		2. Program/Project Title Hot-Gas Cleanup (2.4)		3. Reporting Period 4-1-92 through 6-30-92	
4. Name and Address Energy and Environmental Research Center University of North Dakota Box 8213, University Station Grand Forks, ND 58202 (701) 777-5000				5. Program/Project Start Date 4-1-86	
				6. Completion Date 9-30-92	
Milestone ID. No.	Description	Planned Completion Date	Actual Completion Date	Comments	
Task B	Hot-Gas Particulate Control:				
b.1	Operational tests on HTHP cyclone	11-1-91		Task deleted.	
b.2	Modify sampling equipment	4-1-92			
b.3	Modify hot-gas test loop	10-1-92			
Task D	Alkali Transformation and Interaction Studies:				
d.1	Improve PHOEBE data base	11-1-91	11-1-91		
d.2	Run simulations	2-1-92	3-31-92		
d.3	Perform gettering experiments	3-1-92	5-31-92		
d.4	Perform ceramic protection experiments	6-30-92			
Task E	Semiannual Project Reports:				
e.1	First-half report	1-15-92			
e.2	Second-half report	6-30-92			